The glutaredoxin/glutathione post-stress recovery system is dependent on the availability of glutathione in the cell

By

Erin Blom

BSc. BMedSc. (Hons) Medical Microbiology

Submitted in fulfilment of the academic requirements for the degree of Master of Science in the Discipline of Genetics, School of Life Sciences, College of Agriculture, Engineering and Science, University of KwaZulu-Natal, Pietermaritzburg, South Africa

As the candidate's supervisor, I have approved this dissertation for submission

Supervisor: Dr C.S. Pillay

Signature: _____

Date: __26/06/2020____

Preface

The research contained in this dissertation was completed by the candidate while based in the discipline of Genetics, School of Life Sciences of the College of Agriculture, Engineering and Science, University of KwaZulu-Natal, Pietermaritzburg, South Africa under the supervision of Dr C. S. Pillay.

These studies represent original work by the candidate and have not otherwise been submitted in any form to another University. Where use has been made of the work by other authors it has been duly acknowledged in the text.

Supervisor: Dr C. S. Pillay

Signature: _____

Date: __26/06/2020____

College of Agriculture, Engineering, and Science
Declaration of Plagiarism

I, Erin Blom, declare that:

(i) the research reported in this dissertation, except where otherwise indicated or acknowledged, is my original work;

(ii) this dissertation has not been submitted in full or in part for any degree or examination to any other university;

(iii) this dissertation does not contain other persons' data, pictures, graphs or other information, unless specifically acknowledged as being sourced from other persons;

(iv) this dissertation does not contain other persons' writing unless specifically acknowledged as being sourced from other researchers. Where other written sources have been quoted, then:

a) their words have been re-written, but the general information attributed to them has been referenced;

b) where their exact words have been used, their writing has been placed inside quotation marks, and referenced;

(c) where I have used material for which publications followed, I have indicated in detail my role in the work;

(v) this dissertation is primarily a collection of material, prepared by myself, published as journal articles or presented as a poster and oral presentations at conferences. In some cases, additional material has been included;

(vi) this dissertation does not contain text, graphics or tables copied and pasted from the internet, unless specifically acknowledged, and the source being detailed in the dissertation and in the References sections.

Signature: Erin Blom

Date: 20/05/2020

Declaration Plagiarism 22/05/08 FHDR Approved

Abstract

The cellular response to oxidative stress involves three interconnected processes: reactive oxygen species detoxification, adaptation and repair. Glutathionylation is an adaptive response in which glutathione binds to labile proteins protecting them from oxidative damage but also inactivating them. While it has been established that glutaredoxins play a crucial role in deglutathionylating these proteins, the kinetic regulation of this post-stress repair process is less clear. Intriguingly, aged cells have decreased glutathione levels, although the mechanistic significance of this decrease has not been well-understood. We hypothesized that in these cells, the lower glutathione levels reduced the efficiency of the glutaredoxin/glutathione system which impaired the recovery of the cell post-stress. To test this hypothesis, we used a validated computational model of the glutaredoxin/glutathione system to determine how perturbation of the glutaredoxin system affected the availability of active glutaredoxin as well as the rate of deglutathionylation. We separated the effects of the kinetic and thermodynamic components of glutaredoxin activity and found that the overall flux was primarily controlled by the kinetic effects and that the activity of the system was largely dependent on the availability of reduced glutathione. To test whether reduced deglutathionylation activity was a characteristic of aging, aging and glutathione determination experiments were undertaken in the fission yeast, *Schizosaccharomyces pombe.* In contrast to our hypothesis and data from other studies, fission yeast cells aged for five days were shown to have increased glutathione concentrations, from 36.62 μM to 43.09 μM in minimal media when compared with two-day old cells, except in the presence of additional glutathione or L-buthionine sulfoximine, a glutathione synthesis inhibitor. Further, glutathionylation levels decreased or remained unchanged in the aged cultures which we speculate was due to an adaptive response by the glutathione synthesis pathway in these cells. Future experiments will need to measure both the glutaredoxin system and the metabolic pathways that provide reductive inputs into the system in order to understand the role of the glutathionylation cycle in post-stress recovery.

Acknowledgements

First and foremost, I would like to thank Dr Ché Pillay, my supervisor, for guiding me into a new field and helping me to develop a love for redox biology. Thank you for your support and willingness to read whatever I sent to you – even during the great uncertainty created by COVID-19. Thank you for helping me get to Uruguay to attend my first conference.

Thank you to my team in Lab B23, to Nolyn and Diane for welcoming me and being patient with my never-ending list of questions. To Keli, Lulama, Limpho and Tejal for providing me with many laughs and reminding me that it's always okay to start from scratch.

To Sophia Bam, thank you for your prayers and hilarious moments throughout my university journey. Diane Lind, for convincing me that masters was a must, for helping me navigate the postgraduate world, for patiently teaching me new skills and most importantly for your unwavering friendship and for always having time for me.

Thank you to my grandparents, Les & Ella for backing me in so many ways. Thank you for putting up with my science rants and my stress. I would not be here without your support. To my siblings – Joshua, Julianna, Zack and Seth, thank you for asking me a million questions, for always believing in me and for telling all your friends I was studying to be a doctor.

Thank you to my Dad for stretching my thinking, for never letting me give up and for always believing I was smarter than I am. Thank you to my Mom, Kim, you have sacrificed so much so that I could have the best education, you have helped me fight my self-doubt, you have inspired me to keep going; you are my hero.

To my Lord and Savior Jesus Christ, without You, none of this would even be possible.

List of Abbreviations

ASK1	Apoptosis Signal-regulating Kinase-1
ATP	Adenosine Triphosphate
BCA	Bicinchoninic Acid
BSO	L-Buthionine- (S, R)-Sulfoximine
C_P	Peroxidatic Cysteine
C_R	Resolving Cysteine
CuZnSOD	Copper Zinc Superoxide Dismutase
Cys	Cysteine
DNA	Deoxyribonucleic Acid
DNTB	5,5’ Dithiobis (2-Nitrobenzoic Acid)
DTT	Dithiothreitol
EDTA	Ethylenediaminetetraacetic Acid
EMM	Edinburgh Minimal Media
ETC	Electron Transport Chain
FALS	Familial Amyotrophic Lateral Sclerosis
FeSOD	Iron Superoxide Dismutase
GAPDH	Glyceraldehyde-3-Phosphate Dehydrogenase
Gpx	Glutathione Peroxidase
GR	Glutathione Reductase
Grx	Glutaredoxin
GrxSH	Reduced Glutaredoxin
GrxSHSSG	Glutaredoxin Mixed Disulfide
GrxSS	Oxidized Glutaredoxin/Glutaredoxin Disulfide

GSH	Glutathione
GSSG	Glutathione Disulfide
HIV	Human Immunodefiency Virus
H_2O_2	Hydrogen Peroxide
kDa	Kilodalton
MDA	Malondialdehyde
MetO	Methionine Sulfoxide
$MgCl_2$	Magnesium Chloride
MnSOD	Manganese Superoxide Dismutase
MSR	Methionine Sulfoxide Reductase
NADH	Nicotinamide Adenine Dinucleotide
NADPH	β-Nicotinamide Adenine Dinucleotide Phosphate
NDA	2,3 Naphthalenedicarboxaldehyde
NiSOD	Nickel Superoxide Dismutase
O_2^-	Superoxide Radical
OD_{600}	Optical Density at 600 nm
OH-	Hydroxyl Radical
Pap1	AP-1-like Transcription Factor
PfGrx	*Plasmodium falciparum* Glutaredoxin
Prx	Peroxiredoxin
PSH	Reduced Protein
PSSG	Protein Disulfide / Glutathionylated Protein
PySCes	Python Simulator of Cellular Systems
RNR	Ribonucleotide Reductase

ROS	Reactive Oxygen Species
SDS-PAGE	Sodium Dodecyl Sulfate-Polyacrylamide Gel Electrophoresis
SeCys	Selenocysteine
SOD	Superoxide Dismutase
TB	Tuberculosis
TBA	Thiobarbituric Acid
TBARS	Thiobarbituric Acid Reactive Substances Assay
TCA	Trichloroacetic Acid
Tpx1	Thioredoxin Peroxidase 1
Trx	Thioredoxin
Ura4	Orotidine 5'- Phosphate Decarboxylase
UV	Ultraviolet Radiation
YE	Yeast Extract

Contents

List of Tables

List of Figures

Chapter 1: Literature Review

Oxidative stress is the imbalance between reactive oxygen species (ROS) and antioxidants, and has been linked to the development of numerous diseases – including cancer, diabetes, cardiovascular disease, and age-related diseases such as Alzheimer's disease (Halliwell and Gutteridge, 2015). Significantly, age-related diseases are becoming progressively more prevalent as life expectancy within the global population increases (Atella et al., 2019). The top five causes of mortality amongst the South African population are tuberculosis (TB), diabetes mellitus, non-ischemic heart disease, cerebrovascular diseases, and HIV (Maluleke, 2018). The natural causes of death amongst the over sixty-six age group no longer include communicable diseases such as HIV and TB, but instead include lifestyle and age-related diseases such as cerebrovascular disease, diabetes mellitus, hypertensive diseases, ischemic and other forms of heart disease (Maluleke, 2018). All top five natural causes of mortality are exacerbated by oxidative stress and the correlation between age-related disease and oxidative stress has led to the question of causality. The oxidative stress theory of aging, originally called the free radical theory of aging, was proposed by Denham Harman in 1956 and stated that accumulated oxidative damage is the cause of age-associated loss of cellular function (Harman, 1956). The exact mechanism for oxidative-induced aging was unclear, but Beckman and Ames postulated that ROS exposure increases with age causing defense systems to become overwhelmed (Beckman and Ames, 1998; Liguori et al., 2018). There is also evidence of age-related decline in cellular levels of critical antioxidant molecules such as glutathione, which is also associated with disease development (Zhu et al., 2006). Treatment or supplementation with antioxidants, such as vitamin C, was proposed as a solution, but numerous studies have shown little to no benefit from antioxidant supplementation and thus the causal relationship between ROS and aging remains unclear (McCance et al., 2010; Traber and Stevens, 2011). In this thesis, we hypothesize that the answer may lay in the adaptive and post-stress recovery period rather than the initial exposure to and detoxification of reactive oxygen species. Specifically, we hypothesize that as cells age, the post-stress recovery systems such as methionine sulfoxide reductase and glutaredoxins, become less active, leading to an increase in age-related dysfunction and therefore disease. In order to understand this, one needs to understand the causes and effects of oxidative stress on the cell and the cellular response to it.

1.1: Endogenous & exogenous sources of reactive oxygen species

As a major terminal electron acceptor, oxygen allows for the generation of large amounts of energy in the form of ATP, through oxidative phosphorylation in the electron transport chain (ETC) (Burton and Jauniaux, 2011). In addition to energy generation, certain oxygen-dependent reactions are required by the cell, such as D-amino acid oxidation and the synthesis of collagen I, II and IV (Kalyanaraman, 2013; Halliwell and Gutteridge, 2015; Jain, 2017). Despite the essential nature of these processes, an unfortunate by-product of these reactions is often reactive oxygen species.

Reactive oxygen species (ROS), which include superoxide, hydrogen peroxide and the hydroxyl radical, are oxygen-derived species that are more reactive than oxygen (Halliwell and Gutteridge, 2015; Sies et al., 2017) (Figure 1.1). ROS can result from both endogenous processes and exogenous sources (Ghezzi et al., 2017). The electron transport chain is largely responsible for the leakage of electrons which react with singlet oxygen to produce both superoxide and hydrogen peroxide (Zhao et al., 2019) (Figure 1.1).

$$O_2 \xrightarrow{1e} O_2^{\cdot} \xrightarrow{1e} H_2O_2 \xrightarrow{1e} {}^{-}OH \xrightarrow{1e} H_2O$$

Figure 1.1: Reactive oxygen species development sequence. *Superoxide is formed when molecular oxygen loses a single electron, often as a result of leakage from the electron transport chain (ETC). As the path continues, the oxygen molecule loses a total of four electrons, and along the way, this leads to the formation of hydrogen peroxide, the hydroxyl radical, and lastly, water.*

Other sources of superoxide ($O_2^{-\bullet}$) are NADPH oxidases, peroxidases, and cytochrome P450 (Gan et al., 2011). Despite the fact that superoxide is comparatively less reactive than other ROS such as the hydroxyl radical, individuals lacking the enzyme that detoxifies superoxide, namely superoxide dismutase, are more likely to develop diseases such as Alzheimer's disease and amyotrophic lateral sclerosis (De Belleroche et al., 1995; Beckman et al., 2001; Venkateshappa et al., 2012). Hydrogen peroxide, which is also produced by NADPH oxidases and by the dismutation of superoxide by superoxide dismutases, has the ability to rapidly diffuse from the site of generation, resulting in damage to cellular components (Stöcker et al., 2018). The hydroxyl radical is the most reactive of the three ROS discussed, with reactivity that is diffusion-limited (Möller et al., 2019). In addition

to the endogenous sources listed above, there are exogenous sources of ROS include UV radiation, chemicals, diet, tobacco and infectious agents (Figure 1.2) (Halliwell and Whiteman, 2004).

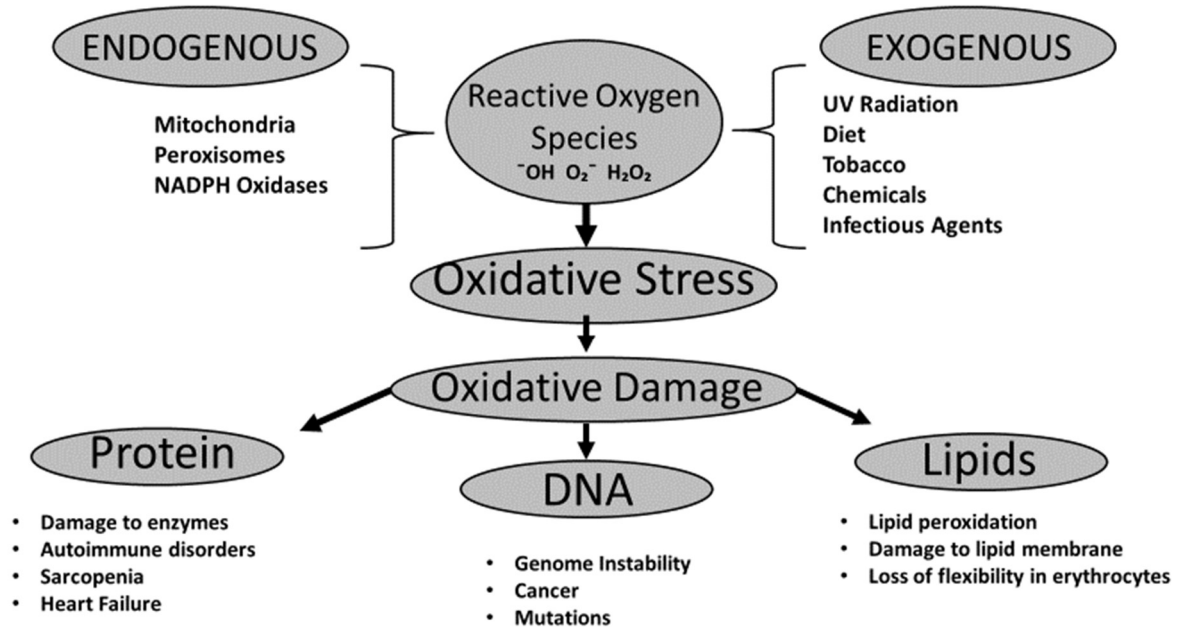

Figure 1.2 Endogenous & exogenous sources of reactive oxygen species and their effects. *Sources of ROS include the mitochondria, peroxisomes and NADPH oxidases (endogenous) and UV radiation, diet and tobacco (exogenous). Adapted from Halliwell and Gutteridge (2015)*

Oxidative stress can result in oxidative damage to important cellular components such as nucleic acids, lipids and proteins (Figure 1.2) (Halliwell and Whiteman, 2004; Halliwell and Gutteridge, 2015; Sies et al., 2017). Accumulation of oxidative damage to cells results in disease which is discussed further in the following sections.

1.2: Roles of reactive oxygen species in disease

There are numerous diseases that result from oxidative damage to proteins (e.g.) cysteine oxidation can result in increased disulfide bridge formation which has been associated with the development of numerous diseases including chronic kidney failure, cystic fibrosis, heart disease and is a key factor in HIV/AIDS disease progression (Zabel et al., 2018; Bennett, 2019; Kamruzzaman et al., 2019). Similarly, protein carbonylation is an irreversible form of protein damage due to direct oxidation of the amino acids lysine, arginine, proline,

and threonine (Berlett and Stadtman, 1997). A meta-analysis of studies investigating the role of oxidative stress in Alzheimer's disease, found increased protein carbonylation in the hippocampus and occipital lobe in individuals known to have Alzheimer's disease when compared to healthy individuals (Zabel et al., 2018).

Oxidative damage to the sugar backbone of DNA can also result in strand breakages, and DNA oxidation is a leading cause of genomic instability, leading to diseases, such as cancer (Tubbs and Nussenzweig, 2017). In DNA, guanine is readily oxidized to 8-oxoguanine, which causes post-replication transversion mutations as a result of incorrect base pairing (Chalissery et al., 2017) which can lead to mitochondrial dysfunction for example (Lee et al., 2004). One of the most well-studied results of oxidative damage to DNA is the shortening of the telomeric region, which is considered to be the general marker of aging (Cattan et al., 2008). In a 2008 study, 14 week old wild-type CAST/Ei mice were exposed to high levels of L-buthionine sulfoximine (BSO), which is a chemical known to chronically deplete glutathione antioxidant levels (Cattan et al., 2008). Tissue glutathione and protein carbonylation were tested in the kidney, liver and heart tissue. BSO-exposed mouse tissues showed a decline in glutathione and an associated increase in protein carbonylation. Exposed mice were also found to have accelerated telomere shortening in multiple tissues, including the testes with an average decrease in telomere length of 15% (Cattan et al., 2008) which led researchers to conclude that oxidative damage to the DNA may be responsible for telomere shortening (Cattan et al., 2008; Zabel et al., 2018). This was of interest as it has previously been shown that oxidative damage to DNA is exacerbated by aging; but the mechanisms behind this remained uncertain (Kujoth et al., 2005; Barnes et al., 2019).

Oxidative damage to lipids results in lipid peroxidation which has two broad consequences- the degradation of membrane integrity and the formation of highly reactive aldehydes (Bradley et al., 2010) A common example of membrane degradation occurs in the erythrocyte membrane which results in loss of cell flexibility, preventing erythrocytes from fitting into small capillaries resulting in decreased blood flow and decreased tissue oxygenation (Srour et al., 2000). The reactive aldehyde byproducts include malondialdehyde, hydroxynonenal, and acrolein which are frequently used as markers of oxidative stress levels (Bradley et al., 2010; Zabel et al., 2018). The first evidence associating lipid peroxidation markers with disease was in a 1994 study by Balasz and Leon where brain tissue obtained from recently deceased individuals known to have Alzheimer's disease was assayed by the thiobarbituric acid reactive substances assay (TBARS) to determine for malondialdehyde levels. This assay involved the reaction of colorless malondialdehyde (MDA) with

thiobarbituric acid (TBA) to produce a red MDA-TBA adduct which was measured photometrically at 530 nm (Balazs and Leon, 1994). A significant increase in malondialdehyde in the hippocampus, frontal and temporal lobes was found in Alzheimer's individuals when compared with age-matched controls (Balazs and Leon, 1994; Zabel et al., 2018). In summary, there is a wealth of evidence that ROS affects proteins, DNA and lipids and this damage has been associated with diseases such as cancer and Alzheimer's disease in both mouse and human studies. To counteract the effects of ROS, there is a cellular response which limits both ROS and oxidative damage.

1.3: The three-stage cellular response to reactive oxygen species

Broadly, the cellular response to ROS consists of detoxification of ROS, ROS-dependent adaptation, and post-stress recovery or repair mechanisms (Figure 1.3). Upon ROS exposure, a range of detoxification mechanisms begin to decrease the ROS load. However, continuous ROS exposure triggers adaptive responses, which include transcription factor activation and post-translational modifications to protect cellular components. Once the ROS levels are under control, it is vital that the cell begins to recover from the oxidative stress.

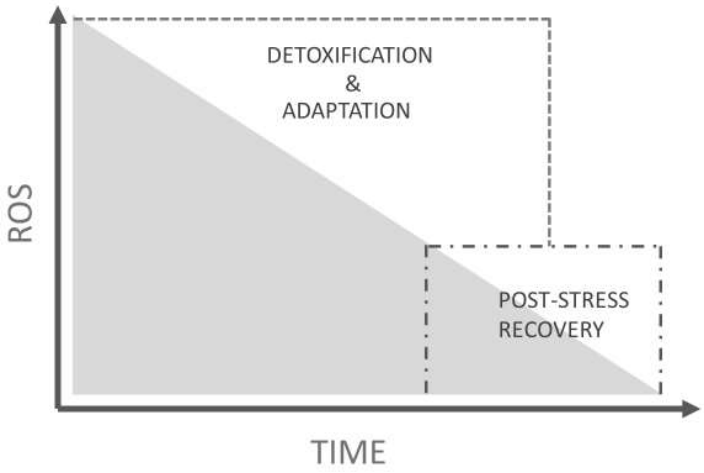

Figure 1.3: A three-part cellular response to reactive oxygen species. *The influx of reactive oxygen species (ROS) activates the cellular response, which encompasses the detoxification, adaptation. As the ROS stress dissipates, the post-stress recovery system is responsible for restoring homeostasis.*

The following paragraphs will explain how the cell attempts to counteract ROS and oxidative damage by means of this three-stage response (Figure 1.3).

1.4: Detoxification

Cells are equipped with an extensive antioxidant defense system for the detoxification of different ROS. Of particular interest are superoxide dismutases (SOD), peroxiredoxins (Prx), catalases, and glutathione peroxidases (Gpx) as they target two of the most prevalent ROS, superoxide and hydrogen peroxide (Figure 1.4).

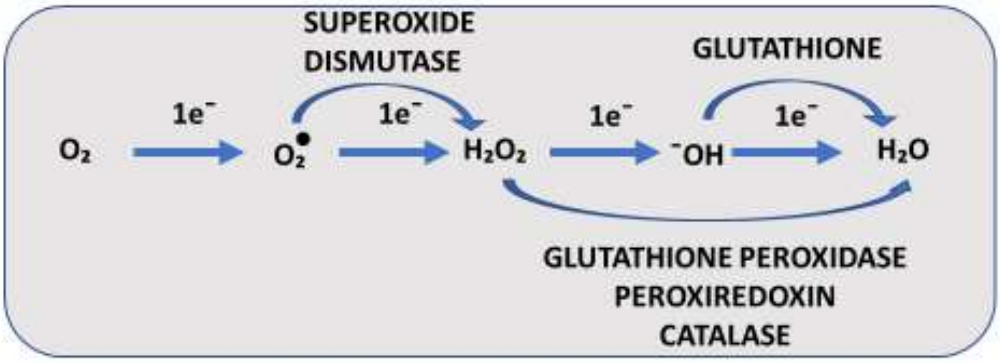

Figure 1.4: An overview of the detoxification stage of cellular defense. *Superoxide dismutase converts superoxide to hydrogen peroxide, which is detoxified by peroxiredoxins, catalases, and glutathione peroxidases. The hydroxyl radical is formed as an intermediate of hydrogen peroxide detoxification and is subsequently detoxified by glutathione.*

1.4.1 Superoxide dismutase

There are a number of SODs in cells, which are named according to the metal cofactor found in the active site, e.g., CuZnSOD, FeSOD, MnSOD and NiSOD (Kernodle and Scandalios, 2001; Banerjee et al., 2008; Ighodaro and Akinloye, 2018). MnSOD, which is also called SOD2, is located in the mitochondria in higher eukaryotes and is of particular interest as the mitochondria are a major source of superoxide ($O_2^{-\bullet}$) (Indo et al., 2015).

The function of superoxide dismutase is to catalyze the conversion of two superoxide molecules to molecular oxygen and hydrogen peroxide (H_2O_2) (Figure 1.5) which is then converted to water by catalase and peroxidases (Haeng-Im et al., 2002; Ighodaro and Akinloye, 2018), (see sections 1.4.2 and 1.4.3 below). SOD catalyzes the dismutation of superoxide at a rate constant of approximately 10^9 $M^{-1}s^{-1}$ which is significantly higher than spontaneous dismutation rate of 10^5 $M^{-1}s^{-1}$ (Azadmanesh and Borgstahl, 2018).

$$2O_2^{-\bullet} + 2H_3O^+ \xrightarrow{Superoxide\ Dismutase} O_2 + H_2O_2 + 2H_2O$$

Figure 1.5: Overall reaction catalyzed by superoxide dismutase. *Superoxide dismutase catalyzes the reaction between two molecules of superoxide, resulting in the formation of molecular oxygen, hydrogen peroxide and two molecules of water.*

Saccharomyces cerevisiae mutants lacking cytosolic SOD1 and mitochondrial SOD2 have decreased growth and increased basal mutation rates when compared to wild-type cells (Das et al., 2018). Previous studies have shown that while SOD2 makes up only 10% of the total yeast SOD, cells lacking SOD2 were highly sensitive to oxygen and ethanol (Longo et al., 1999). However, more recent studies have demonstrated that the SOD1 is responsible for the majority of SOD activity. A study comparing wild-type and mutant mice lacking SOD1 and found that SOD1 knockout mice aged significantly faster than wild-type mice and had a 30% decrease in lifespan (Muller et al., 2006). The protein carbonyls present in the skeletal muscle plasma increased by 45% in the SOD1 mutant mice when compared with the wild type mice (Muller et al., 2006; Deepa et al., 2019).

Glutathionylation is a post-translational modification that is promoted by oxidative stress (discussed below) and can reduce the activity of proteins (Yamakura and Kawasaki, 2010). To investigate the impact of glutathionylation on the dimeric stability of SOD1, Wilcox *et al* (2009), used size exclusion chromatography to compare normal and glutathionylated SOD1 from human erythrocytes. It was found that glutathionylation promoted the formation of SOD1 dimers and thus led to the aggregation associated with familial amyotrophic lateral sclerosis (FALS), a fatal disease characterized by motor neuron loss (Wilcox et al., 2009; Yamakura and Kawasaki, 2010).

1.4.2 Peroxiredoxins

Peroxiredoxins are a family of cysteine-based enzymes found across all kingdoms, with the shared active site motif PxxTxxC (Wong et al., 2004; Perkins et al., 2015). Peroxiredoxins exist in six evolutionary subfamilies (Prx1, Prx5, Prx6, Tpx, PrxQ, and AhpE); all six are present in prokaryotes whilst only Prx1, Prx5, Prx6, and PrxQ subfamilies are present in eukaryotes. In simple eukaryotes, such as the model organism *Schizosaccharomyces pombe*, there is one peroxiredoxin, while in the budding yeast *S. cerevisiae* there are five, four of which bear strong similarity with four of the six mammalian peroxiredoxins (Wong et al., 2004). Peroxiredoxins are responsible for protection from

oxidative stress, being one of the two major enzymatic defenses against H_2O_2 with the other being catalase.

In terms of defense, peroxiredoxins have been shown to reduce up to 90% of cellular peroxides, due to their high concentrations and reactivity (10^6-10^8 M^{-1} s^{-1}) (Peskin et al., 2007). Peroxiredoxins possess a tertiary structure that allows the active site to be highly specific to hydrogen peroxide which facilitates their ability to be effective at nanomolar concentrations of hydrogen peroxide (Peskin et al., 2007; Trujillo et al., 2007; Winterbourn, 2008).

The conserved active site cysteine residue on peroxiredoxins is known as the peroxidatic cysteine (C_P) (Rhee, 2016) and is oxidized by hydrogen peroxide, resulting in the formation of cysteine sulfenic acid, which then reacts with another cysteine, known as the resolving cysteine (C_R) to form two molecules of water and a disulfide (Figure 1.6). The inactive enzyme is reduced by thioredoxin and thioredoxin reductase (Peskin et al., 2013a; Rhee, 2016)

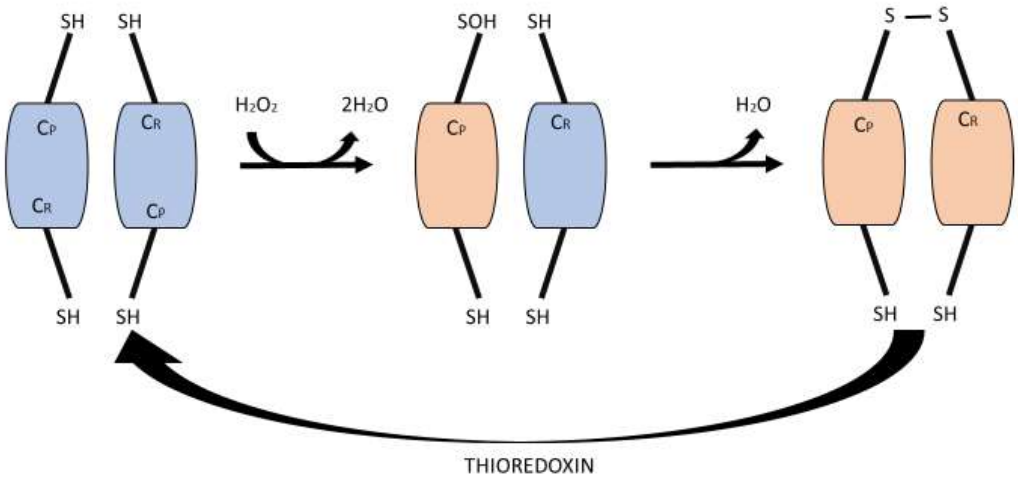

Figure 1.6 Mechanism of hydrogen peroxide detoxification by typical 2-cys peroxiredoxins. *The peroxidatic cysteine (Cp) is oxidized by hydrogen peroxide and reacts with the resolving cysteine (Cr) resulting in the formation of water and a disulfide. Thioredoxin reduces the disulfide to reactivate the peroxiredoxin. Adapted from Sharapov et al (2014).*

The effect of deleting all five Prxs and three glutathione peroxidases in *S. cerevisiae* was compared with wild type and a number of different single peroxiredoxin delete strains (Kaya et al., 2014). These strains were grown on complex media and DNA was isolated and sequenced using Illumina sequencing. When compared with the wild type sequence, 2633

point mutations were observed in the yeast strain lacking all peroxiredoxins and peroxidases but only 24 in the strain lacking glutathione peroxidase and 91 in the strain lacking all five peroxiredoxins (Kaya et al., 2014). This work also showed that yeast strains lacking all five peroxiredoxins were more sensitive to ROS but were still viable due to the effects of other antioxidants, such as catalase (Wong et al., 2004).

1.4.3 Catalase

Catalases are 240 kDa enzymes that comprise four subunits of 60 kDa, each of which contain ferroprotoporphyrin (Ighodaro and Akinloye, 2018). Present in all living organisms that utilize oxygen, catalase is one of the most prolific antioxidants. Human erythrocytes, in particular, contain catalase to protect them from hydrogen peroxide formed during hemoglobin autooxidation. Erythrocytes can also protect other cells from hydrogen peroxide damage by absorbing it and allowing the catalase to process it (Halliwell and Gutteridge, 2015; Morabito et al., 2019).

Catalase requires an iron cofactor to catalyze the degradation of hydrogen peroxide into molecular oxygen and water (Ighodaro and Akinloye, 2018). Exposure to a hydrogen peroxide molecule results in the oxidation of the heme group in the catalase, leading to the formation of a porphyrin cation. The enzyme is returned to resting-state by a second hydrogen peroxide molecule, which acts as a reducing agent and results in the production of water and oxygen (Figure 1.7) (Ighodaro and Akinloye, 2018). Unlike peroxiredoxins, catalase works to directly decompose two molecules of hydrogen peroxide to two molecules of water and oxygen (Aebi, 1984). Catalases have a much lower affinity for hydrogen peroxide than Prxs and are most effective at high concentrations of hydrogen peroxide, which is why Prxs are responsible for the majority of hydrogen peroxide detoxification under normoxic conditions (Rhee et al., 2005; Rhee, 2016).

$$2H_2O_2 \xrightarrow{Catalase} 2H_2O + O_2$$

Figure 1.7: Decomposition of hydrogen peroxide by catalase. *Catalase catalyzes the decomposition of two molecules of hydrogen peroxide into two molecules of water and molecular oxygen.*

Catalase deficiency, acatalasemia or hypocatalasemia, has been associated with an increase in Type 2 diabetes, reflecting the sensitivity of pancreatic β cells to hydrogen

peroxide, which is produced by the mitochondria in β cells (Goth and Eaton, 2000). This was confirmed in a mouse study, which showed that catalase deletion resulted in prediabetic conditions in mice (Heit et al., 2017). Specifically, catalase knockout mice showed impaired glucose tolerance, increased fasting serum insulin levels and increased obesity, all of which are consistent with pre-diabetes (Heit et al., 2017).

1.4.4 Glutathione peroxidase

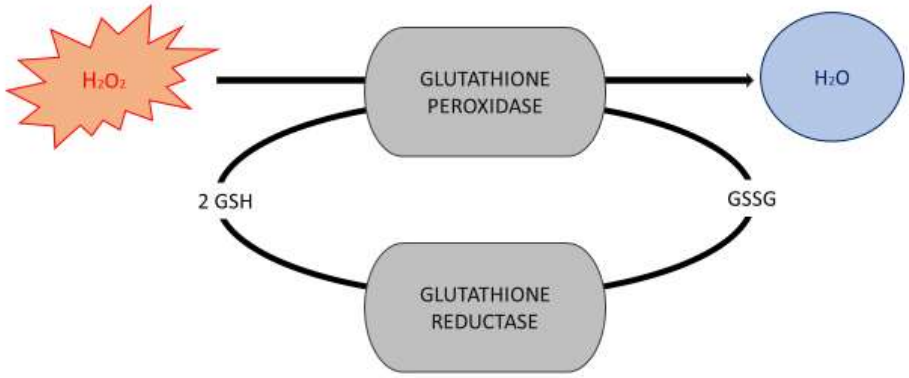

Figure 1.8: Glutathione peroxidase catalyzes the reduction of hydrogen peroxide to water. *The glutathione peroxidase relies on reduction by glutathione (GSH), which leads to the formation of glutathione disulfide (GSSG), which is the oxidized form of glutathione. Glutathione reductase completes the system by reducing GSSG to GSH. Adapted from (Pinto et al., 2002).*

Glutathione peroxidase (Gpx) has a similar function to that of Prx, as it catalyzes the reduction of hydrogen peroxide to water (Figure 1.8) (Dayer et al., 2008). Gpx was discovered as an enzyme that protected human erythrocyte from oxidative damage (Mills, 1957). Gpx exists in in two forms – selenocysteine (SeCys)-Gpx, which contains a SeCys residue at the active site and is found in humans and most mammals, and non-selenocysteine (NS)-Gpx, which has a cysteine residue in the active site and is found in yeasts, plants and some animals (Dayer et al., 2008). SeCys-Gpx is reduced by reduced glutathione whilst NS-Gpx, the Gpx in yeast is reduced by thioredoxin, making NS-Gpx even more similar to Prx (Tanaka et al., 2005). GPx deficiency can result in the development of vascular oxidative stress and cancers, and this is believed to be due to the oxidative damage to both functional proteins and membrane fatty acids (Ighodaro and Akinloye, 2018).

1.5 Adaptive response

Adaptation, which occurs in conjunction with detoxification, includes both transcriptional and post-translational modifications such as glutathionylation. (Sies, 2018). These adaptive responses allow cells to adapt to the presence of ROS by two mechanisms: (i) activating the transcription factors required for defense system activation by redox signaling and (ii) by protecting vulnerable protein components from damage.

1.5.1 Redox signaling

Redox signaling pathways play important roles in cell proliferation, DNA synthesis and apoptosis. Briefly, cell signaling is defined as being a process by which information is transmitted into the nucleus to allow for important biological functions, usually in response to the external stimuli, to occur (Arkun and Yasemi, 2018). Below, three types of redox signaling are considered: direct sensor signaling, sensor-mediated signaling and indirect signaling which form part of the cellular response to ROS and oxidative stress (Pillay et al., 2016).

1.5.1.1 Direct sensor signaling

Direct sensor signaling is an adaptive response that occurs when the transcription factor is directly oxidized; the classic example of this is the oxidation of *E. coli* transcription factor, OxyR (Åslund et al., 1999). Briefly, OxyR is activated when exposed to hydrogen peroxide, which causes the formation of an intramolecular disulfide bond between cysteine residue 199 and 208 (Åslund et al., 1999). OxyR is responsible for activating the transcription of the genes for antioxidant defense systems, such as glutathione reductase, glutaredoxin 1, and hydroperoxidase 1 and catalase (Netto and Antunes, 2016). It was shown that glutathionylation is also a mechanism of OxyR activation and OxyR is deactivated when it is reduced by glutaredoxin 1 (Kim et al., 2002).

1.5.1.2 Sensor-mediated signaling

Sensor-mediated signaling involves the presence of a sensor molecule that becomes oxidized by hydrogen peroxide for example, and is then responsible for activating a transcription factor (Pillay et al., 2016). In addition to their role in directly detoxifying hydrogen peroxide, peroxiredoxins play this role in the adaptive response to ROS through the regulation of cell signaling (Perkins et al., 2015). An example of this is the thiolperoxidase 1 (Tpx1)–Pap1 pathway in *S. pombe* (Paulo et al., 2014). Tpx1 is a member of the peroxiredoxin family which is present in *S. pombe* and when oxidized, transmits oxidizing equivalents to

Pap1 an AP 1-like transcription factor which initiates the transcription of antioxidant genes (Figure 1.9). Pap1 activation is most effective over low to intermediate concentrations of hydrogen peroxide (~0.2 mM-1 M), However, at higher concentrations of hydrogen peroxide, Pap1 activation is delayed by ~30 minutes as Tpx1 becomes hyperoxidized (Vivancos et al., 2005).

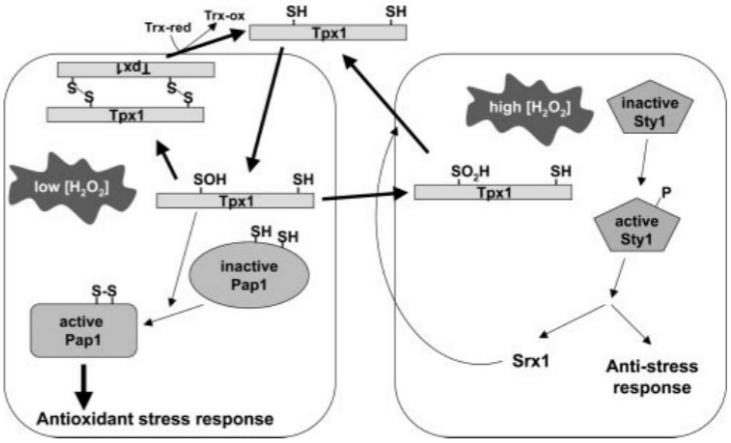

Figure 1.9 Model of the Pap1 activation pathway in low versus high hydrogen peroxide conditions. *Under low concentrations of hydrogen peroxide (left), the inactive Pap1 becomes oxidized and activated by the oxidized Tpx1, initiating an antioxidant stress response. However, in the presence of high concentrations of hydrogen peroxide, Tpx1 becomes hyperoxidized and the Sty1 general stress response pathway is activated, leading to the activation of sulfiredoxin (Vivancos et al., 2005) (Copyright permission granted by PNAS).*

1.5.1.3 Indirect signaling

Indirect signaling is a secondary redox signaling mechanism. An example of this type of signaling is when significant peroxiredoxin oxidation leads to concomitant thioredoxin oxidation, resulting in a signaling event. An example of indirect redox signaling is the mammalian apoptosis signal-regulating kinase-1 (ASK1)/thioredoxin (Trx) pathway. ASK1 is a stress signaling complex that responds to increased ROS in the cellular environment and it is inhibited by Trx1, which is an important antioxidant. Under normal conditions, Trx1 is attached to ASK1 but under oxidative stress, Trx1 becomes oxidized by Prx1 and is detached from ASK1. This results in the formation of ASK1-ASK1 oligomers and the activation of the ASK1 signaling cascade, leading to apoptosis (Latimer and Veal, 2016).

1.5.2 Glutathione and glutathionylation

Glutathione (GSH) is an abundant low molecular weight thiol antioxidant, existing in most eukaryotes and Gram-negative bacteria. GSH is comprised of the tripeptide γ-L-glutamyl-L-cysteinyl-glycine and is synthesized in a two-step process, with the first step being the formation of a peptide bond between glutamate and cysteine catalyzed by glutamate-cysteine ligase. The second step, catalyzed by glutathione synthetase, is the addition of the glycine residue (Figure 1.10) (Morris et al., 2014a; Giustarini et al., 2016). Interestingly, there are alternative low molecular weight thiols present in some organisms, for example *Trypanosoma brucei* synthesizes trypanothione by cross-linking two GSH molecules with spermidine while mycothiol is utilized by most *Actinomycetes*, including *Mycobacterium tuberculosis* (Flohe et al., 1999; Hugo et al., 2018; Reyes et al., 2018).

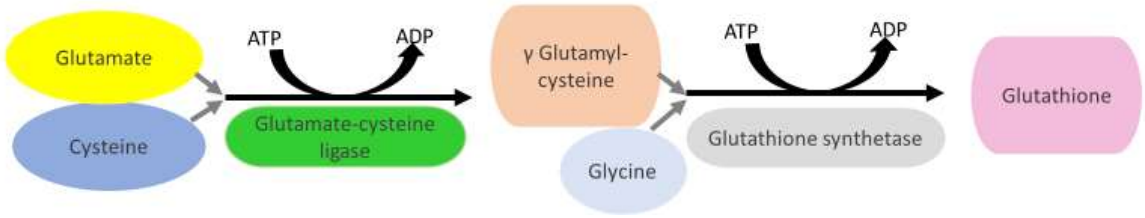

Figure 1.10: Synthesis of glutathione by γ-glutamate-cysteine ligase & glutathione synthetase. *The two-step process of glutathione synthesis requires two molecules of ATP, the amino acids glutamate, cysteine and glycine, and enzymes γ-glutamate-cysteine ligase & glutathione synthetase. Adapted from (Giustarini et al., 2016).*

Under normal conditions, intracellular glutathione exists predominantly in the reduced form, GSH, (Mieyal et al., 2008; Ballatori et al., 2009) with intracellular concentrations as high as 20 mM in *E. coli* and 13 mM in yeast (Deponte, 2017). This high intracellular concentration had led to GSH being considered the most important cellular redox buffer (Schafer and Buettner, 2001; Deponte, 2017). Upon oxidation, GSH becomes oxidized to GSSG as electrons are donated from the sulfur atoms of two GSH groups (Giustarini et al., 2016). Thus, a decrease in GSH results in an increase in GSSG, which is why the GSH/GSSG ratio has been proposed as an indicator of redox state (Schafer and Buettner, 2001; Giustarini et al., 2016) and changes in this couple have been correlated with cell proliferation, differentiation and apoptosis (Ballatori et al., 2009).

Table 1.2 Consequences of the glutathionylation of some important proteins

Protein	Consequence	Reference
GAPDH	Inhibition of enzyme activity	(Ravichandran et al., 1994)
Actin	Decreased polymerization	(Wang et al., 2001)
STAT3	Inhibition of signaling	(Xie et al., 2008)
PTP1B	Inhibited phosphatase activity	(Barrett et al., 1999)
c-jun, NFkBp50	Inhibition DNA biding	(Klatt et al., 1999)
Na (+)–K (+) pump	Inhibition of pump activity	(Deponte, 2017)

Numerous *in vitro* studies have shown that oxidative stress can lead to the peroxidatic cysteine of peroxiredoxins becoming glutathionylated (Radyuk and Orr, 2018). For example, it was shown that *in vitro* exposure to hydrogen peroxide could result in the glutathionylation of Prx2 (Peskin et al., 2016). *In vivo* studies have since showed an accumulation of glutathionylated Prx2 in mice lacking glutaredoxin 1 (Peskin et al., 2016; Radyuk and Orr, 2018). There are a number of human pathologies that result from glutathionylation including iron deficiency anemia where hemoglobin is glutathionylated, Alzheimer's disease in which glutathionylated targets include enolase and GAPDH, and atherosclerosis where serum proteins become glutathionylated. The glutathionylation of serum proteins in individuals with atherosclerosis was shown in a study that took serum samples from 41 patients previously diagnosed with atherosclerosis and subjected the sample to detection by biotin glutathione S-transferase on blotted membranes. Statistical analysis revealed a significant increase in glutathionylated serum proteins in patients diagnosed with atherosclerosis when compared with the control group (Nonaka et al., 2007).

There is still debate around why GSH is so important for cell survival, including the proposal that in certain organisms, such as yeast, GSH is vital for iron-sulfur cluster formation and not for antioxidant defense (Deponte, 2017; Toledano and Huang, 2017). There is also still debate about the reason for the high concentrations of GSH present in the cell (Deponte, 2017). The contradictory data has led us to ask whether the high concentrations of GSH may in fact be more important in the post-stress recovery stage of the cellular response, which is discussed in the subsequent sections.

Table 1.1: Age-related decrease in glutathione levels

Organism (Tissue)	% Decrease in GSH	Age Range	Reference
Rat (Brain)	25	4-17 months	(Zhu et al., 2006)

Fruit Fly	36.5	2-27 days	(Sohal et al., 1990)
Human (Erythrocyte)	7.03	40-69 years	(Gil et al., 2006)
Human (Whole Blood)	15.99	40-69 years	(Erden-İnal et al., 2002)

A decrease in cellular GSH in humans results in an increased potential for inflammation as well as lower levels of DNA synthesis and cell proliferation, especially in human lung and heart tissue (Rahman and MacNee, 2000; Kamruzzaman et al., 2019) . Of relevance to this study, GSH depletion results in increased levels of oxidative stress and mitochondrial dysfunction – both of which are associated with a number of neuroimmune disorders such as depression and Parkinson's disease, age-related diseases such as glaucoma and age-related cataracts, viral infections such as HIV, cardiovascular disease and diabetes (Mieyal et al., 2008; Morris et al., 2014a). Interestingly, cancer cells appear to have increased levels of GSH which could potentially aid these cells in avoiding apoptosis. During chemotherapy GSH-blockers are therefore given to reduce the protective effects of GSH on the cancer cells as well as the detoxifying effects of GSH on chemotherapeutic drugs (Ballatori et al., 2009). An intriguing correlation between aging and a decline in GSH level has been observed in a number of organisms (Table 1.1), and this relationship has long been used to argue that cells become increasingly more susceptible to ROS damage with age (Di Stefano et al., 2006). However, the significance of the decrease in glutathione is unclear due to the fact that glutathione is present in the millimolar range (Deponte, 2017). In addition, glutathione is expected to play a very limited role in the detoxification of ROS due to its limited reactivity with ROS such as hydrogen peroxide (0.87 M^{-1} s^{-1}) especially considering that specialist redox enzymes such as peroxiredoxins and catalases are far more reactive with rates of up to 10^6-10^8 M^{-1} s^{-1} for peroxiredoxins (Winterbourn and Metodiewa, 1999; Peskin et al., 2007; Giustarini et al., 2016; Deponte, 2017).

The pathologies associated with GSH depletion are likely to due to dysregulation of protein-S-glutathionylation, a process which involves the addition of GSH to a cysteine residue of a protein in the presence of ROS (Figure 1.11). The process results in the formation of a protein mixed disulfide and thereby protecting sensitive thiol residues from oxidative damage (Mieyal et al., 2008; Morris et al., 2014a). In order for a thiol modification to be defined as protein-S-glutathionylation it must: (1) occur at a specific site and alter the activity of the affected protein; (2) occur under physiologically relevant conditions (i.e. high GSH/GSSG ratio); (3) elicit a physiological response to stimulus; (4) be rapid and efficient;

and lastly, (5) have a rapid and efficient mechanism of reversal (Mieyal et al., 2008). Interestingly, two broad mechanisms for protein-S-glutathionylation with a number of intermediates have been proposed (Figure 1.11) (Mieyal et al., 2008). The first proposed mechanism for protein-S-glutathionylation is the thiol-disulfide exchange mechanism, whereby oxidized glutathione combines with reduced protein (Reaction 1, Figure 1.11). The second ROS-mediated mechanism involves the formation of a number of different intermediates which such as sulfenic acid, sulfanilamide, thiyl radical, thiosulfinate or S-nitrosyl modification (Figure 1. 11) (Mieyal et al., 2008). In subsequent years, the dependence of glutathionylation on the availability of GSH has been reinforced, but the exact mechanism of glutathionylation remains to be elucidated (Cha et al., 2017).

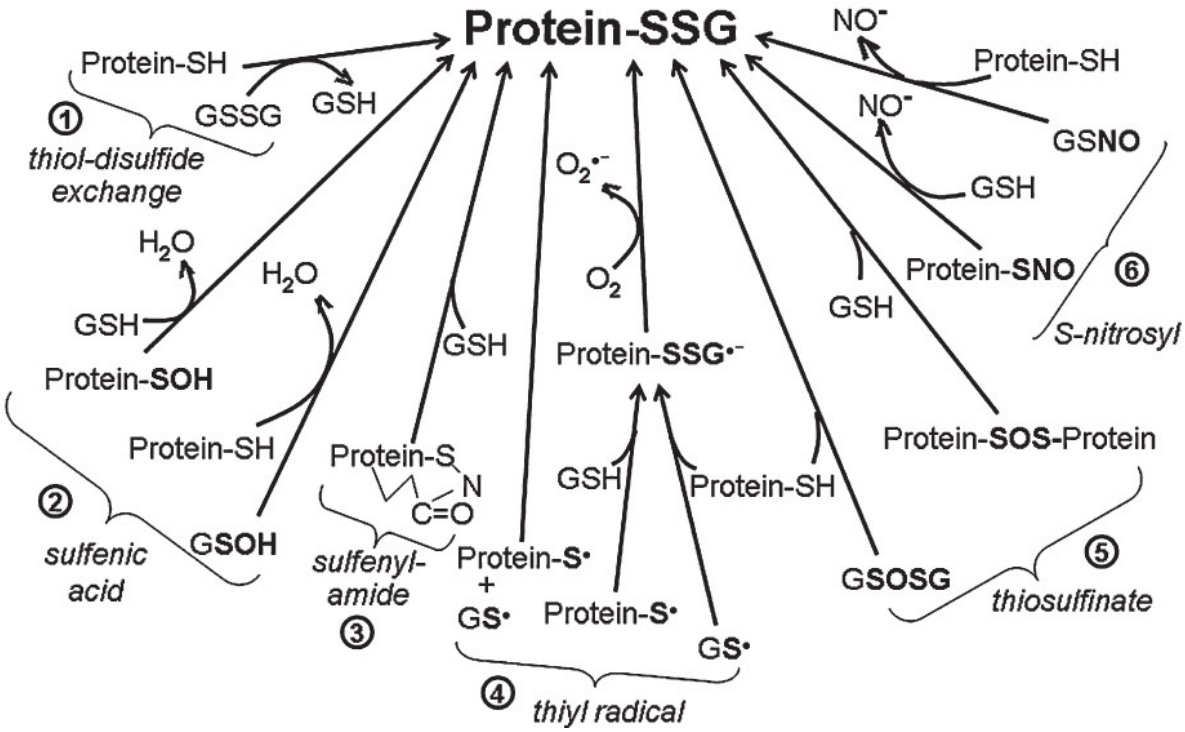

Figure 1.11: Potential mechanisms for protein-S-glutathionylation. *Proposed mechanisms are (1) thiol-disulfide exchange, and via the formation of a number of potential intermediates, (2) sulfenic acid, (3) sulfanilamide, (4) thiyl radical, (5) thiosulfinate and (6) S-nitrosyl respectively (Meiyal et al., 2008). (Copyright permission granted by Mary Ann Liebert Inc.)*

Protein-S-glutathionylation of proteins occurs in two classes, for example, activating, occurring in mitochondrial complex II, HIV-1 protease and OxyR, and deactivating,

occurring in protein kinase A and glyceraldehyde-3-phosphate dehydrogenase (GAPDH) (Lind et al., 1998; Humphries et al., 2002; Morris et al., 2014b). Table 1.2 highlights the importance of deglutathionylation where glutathionylation results in inhibition of activity (e.g.) glutathionylation of GAPDH prevents the enzyme from catalyzing the dehydrogenation of glyceraldehyde-3-phosphatase during glycolysis, which has detrimental effects on glucose metabolism (Cotgreave et al., 2002) and GAPDH inhibition has been associated with the development of insulin resistance, a precursor to diabetes (Wentzel et al., 2003; Sirover, 2017). In addition, accumulation of glutathionylated GAPDH has been observed in brain tissue of individuals with Alzheimer's disease (Newman et al., 2007).

1.6 Post stress recovery

Post-stress recovery or repair takes place, as the name suggests, once the oxidative stress has begun to dissipate. The need for a repair system is largely due to the deactivating effect that many of the oxidants and antioxidants have on cell components like proteins. Post-stress recovery systems facilitate the reactivation of proteins, often by undoing post-translational modifications that occur as a cellular adaptation strategy. Two major systems were considered in this study, namely the methionine sulfoxide reductase and glutaredoxin/glutathione systems.

1.6.1 Methionine sulfoxide reductase

Methionine is an essential amino acid that is not synthesized by mammals (Tarrago and Gladyshev, 2012). Methionine residues on proteins can be readily oxidized by ROS, such as the hydroxyl radical, superoxide, hypochlorous acid, and hypobromous acid, to form methionine sulfoxide (MetO) in two isoforms- R or S (Tarrago and Gladyshev, 2012). Methionine sulfoxide reductase (Msr) was isolated in *E. coli* in 1980 as part of a study which discovered the system responsible for restoring protein activity to proteins with oxidized methionine residues. Methionine sulfoxide reductase is an enzyme vital to the regulation of redox homeostasis, with MsrA enzymes reducing S isoforms, whilst R isoforms are reversed by MsrB enzymes (Moskovitz et al., 2001). Initially, thioredoxin and thioredoxin reductase were thought to be solely responsible for this restoration (Porqué et al., 1970; Achilli et al., 2015). Subsequently, methionine sulfoxide reductase was discovered in almost all forms of life, with the exception of a small number of hyperthermophiles and parasites (Tarrago and Gladyshev, 2012). Interestingly in humans, methionine sulfoxide reductases are more

concentrated in cells exposed to high levels of ROS, such as the immune cells macrophages and neutrophils (Brot et al., 1984; Moskovitz et al., 2000).

The fact that methionine is readily oxidized has led to the suggestion that methionine sulfoxide reductase could have three functions, firstly as a ROS scavenging antioxidant, secondly as a regulator of critical enzyme function and lastly, as a repair system that aims to keep methionine residues in the reduced form (Moskovitz et al., 1997; Moskovitz et al., 2001). MsrA is able to reduce both free MetO and protein-bound MetO, suggesting that the enzyme is also responsible for reclaiming methionine, which may be important for cell survival as both *S. cerevisiae* and *E. coli* mutants lacking *msrA* showed a reduced survival rate (Moskovitz et al., 2001).

MsrA gene deletion studies have been undertaken in numerous eukaryotic organisms, including yeast, *Caenorhabditis elegans* and mice, and all have shown increased oxidative damage and significantly decreased lifespans (Tarrago and Gladyshev, 2012). By contrast, *MsrB* knockout organisms were less sensitive to its depletion, For example, Le *et al*., compared the hydrogen peroxide sensitivity in yeast cells and found that *MsrA* knockouts were more sensitive to the oxidant than the similarly sensitive *MsrB* knockout cells and wild-type yeast cells were (Le et al., 2009).

1.6.2 Glutaredoxins

Glutaredoxins (Grxs) are small (9-14 kDa), heat-stable, GSH-dependent oxidoreductases, and were first discovered as hydrogen donors for ribonucleotide reductase (RNR) (Holmgren, 1976, 1989; Grant, 2001). Ribonucleotide reductases catalyze the synthesis of deoxyribonucleoside diphosphates, which are the precursors to DNA building blocks, deoxyribonucleoside triphosphates (Chen et al., 2019). This reaction requires electrons which are usually provided by dithiol donors. Originally, thioredoxin was believed to be the primary donor until a study testing the impact of *E. coli* mutant cells lacking thioredoxin showed that the ribonucleotide reductases were still functioning which led to the discovery of glutaredoxins (Holmgren, 1976). Glutaredoxins are present in eukaryotes, including both plants and animals, prokaryotes, and certain viruses (Fernandes and Holmgren, 2004).

Glutaredoxins are part of the thioredoxin (Trx) family and therefore share the common Trx-fold structure, hallmarks of which are a *cis*-proline residue located prior to β-sheet three and the C-x-x-C active site motif located on the loop connecting β-sheet one and α-helix one. When compared to thioredoxins, glutaredoxin shows a significant affinity for GSH (Holmgren

et al., 2005; Berndt et al., 2008b). Despite this common Trx motif, two types of glutaredoxins exist, monothiol and dithiol glutaredoxins, which are defined by their active sites (Molina et al., 2004). In monothiol glutaredoxins one of the active site cysteines is replaced with a serine residue and the most commonly occurring active site mutant is cysteine-glycine-phenylalanine-serine (C-G-F-S) (Toledano et al., 2007; Berndt et al., 2008a). Dithiol glutaredoxins have both active site cysteines and most commonly contain a cysteine-proline-tyrosine-cysteine (C-P-Y-C) active site (Holmgren, 1989; Toledano et al., 2007). Glutaredoxin amino acid sequences are highly homologous amongst various species, which allows one to study glutaredoxin mechanisms in less complex organisms and then extend this analysis to higher eukaryotes (Kalinina et al., 2008).

Since their original discovery as hydrogen donors to RNR in *E. coli* cells lacking thioredoxin, glutaredoxins have also been shown to play a role in sulfur metabolism, protein folding, reduction of dihydroascorbate, repairing of oxidative damage in proteins, regulation of transcriptional, metabolic and structural processes (Grant, 2001). However, the most important function of glutaredoxins appears to be deglutathionylation – the reduction of glutathionylated mixed disulfides, using a mechanism that, in principle, requires only the N-terminal active site cysteine (Berndt et al., 2008a). Deglutathionylation restores functionally active thiols, and Grx1 has been shown to deglutathionylate important human proteins such as hemoglobin, nuclear factor 1, and Ras (Figure 1.12) (Chrestensen et al., 2000).

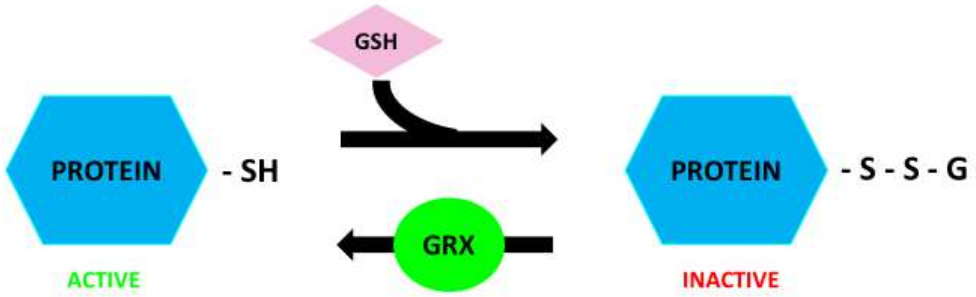

Figure 1.12: Deglutathionylation restores activity to proteins. *Deglutathionylation, the removal of glutathione residues from proteins, is a process catalyzed by glutaredoxins which results in the reactivation of proteins inactivated by glutathionylation.*

The main role of glutaredoxin is to remove glutathione from glutathionylated proteins, and the importance of glutaredoxin in this role has been shown in numerous studies (Mailloux

et al., 2020). However, it has also been shown that under oxidative stress conditions and the presence of excess glutathione thiol, the glutaredoxin reverses it's usual deglutathionylation activity and begins adding glutathione to vulnerable cysteine residues and therefore glutaredoxin may play a role in glutathionylation as well (Liao et al., 2010) as mutants lacking glutaredoxin showed decreased levels of glutathionylation under stressed condition (Liao et al., 2010). The implication of this is that glutaredoxins may play a role in both defense and post-stress recovery or repair. The deglutathionylation activity of glutaredoxin is discussed in Chapter 2.

1.7 Research question

The deglutathionylation activity of glutaredoxin is an important post-oxidative stress recovery/repair system and we hypothesized that this activity is regulated kinetically by the availability of GSH in the system. Secondly, we hypothesized that aging cells would have decreased GSH and consequently their glutaredoxin systems would be less effective. We would therefore expect higher levels of glutathionylated proteins in these cells. The aims and objectives associated with each of these hypotheses is explained in the chapters that follow, where we tested these hypotheses with computational modeling and *in vivo* assays.

Chapter 2: Kinetic modeling of the glutaredoxin/glutathione system

2.1 Introduction

The complex connectivity of redox systems can make their activity difficult to predict which has prompted researchers to utilize computational modeling as an efficient and cost-effective tool to test hypotheses on these systems. A good model provides two crucial functions – the ability to assess consistency within wet-lab data and to facilitate accurate prediction of the behavior of a system. However, a correct model must be based on known reactions and kinetic parameters obtained through wet-lab experimentation and the model's predictive value and integrity should be validated by being compared to realistic datasets (Pillay et al., 2013; Conway, 2019; Medley, 2019). Before a model can be designed or chosen, a schematic diagram of the system is usually used to guide model development (Figure 2.1).

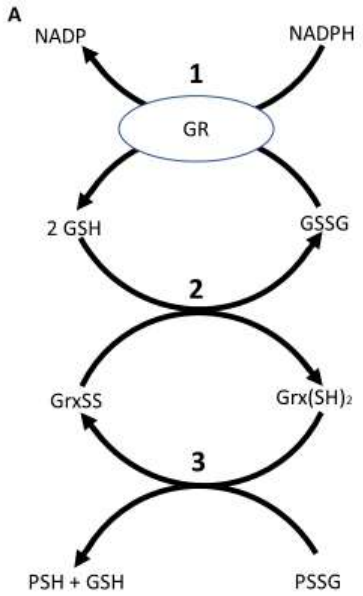

Figure 2.1: Schematic model of the glutaredoxin/glutathione system. *The reactions (from top down): reaction 1 is the reduction of glutathione disulfide (GSSG) to reduced glutathione (GSH) by glutathione reductase, which requires NADPH. Reaction 2 is the reduction of glutaredoxin disulfide (GrxSS) to reduced glutaredoxin ($Grx(SH)_2$) by reduced glutathione. Reaction 3 is the reduction of protein mixed disulfide (PSSG) to reduced protein (PSH) and glutathione (GSH) by reduced glutaredoxin ($Grx(SH)_2$). (Adapted from Pillay et al., 2009).*

Although the glutaredoxin/glutathione reaction scheme only appears to involve three reactions, the kinetic mechanism for glutaredoxin activity have been an area of dispute which has resulted in discrepancies in model formulation. It is crucial that the correct model is used for analyses to ensure that the model's output is valid. Previous work by our group used the glutaredoxin/glutathione schematic diagram (Figure 2.1) to build a reaction scheme for this system:

Scheme I:

$$GSSG + NADPH \rightarrow 2GSH + NADP \quad (1)$$

$$GrxSS + 2\,GSH \rightarrow GrxSH + GSSG \quad (2)$$

$$GrxSH + PSSG \rightarrow GrxSS + PSH + GSH \quad (3)$$

It was previously determined that reduction of glutathione disulfide by glutathione reductase (reaction 1) was irreversible and that the subsequent reactions, reduction of glutaredoxin disulfide by reduced glutathione (2) and deglutathionylation of the protein disulfide by reduced glutaredoxin (3) should be modeled using mass action kinetics, rather than Michaelis-Menten kinetics (Pillay et al., 2009). This approach was validated by fitting to an *in vitro* dataset (Figure 2.2A) and the resulting model was able to predict independent kinetic datasets (Figure 2.2 B & C) (Pillay et al., 2009). Thus, this kinetic model was determined to be an accurate representation of the glutaredoxin/glutathione system.

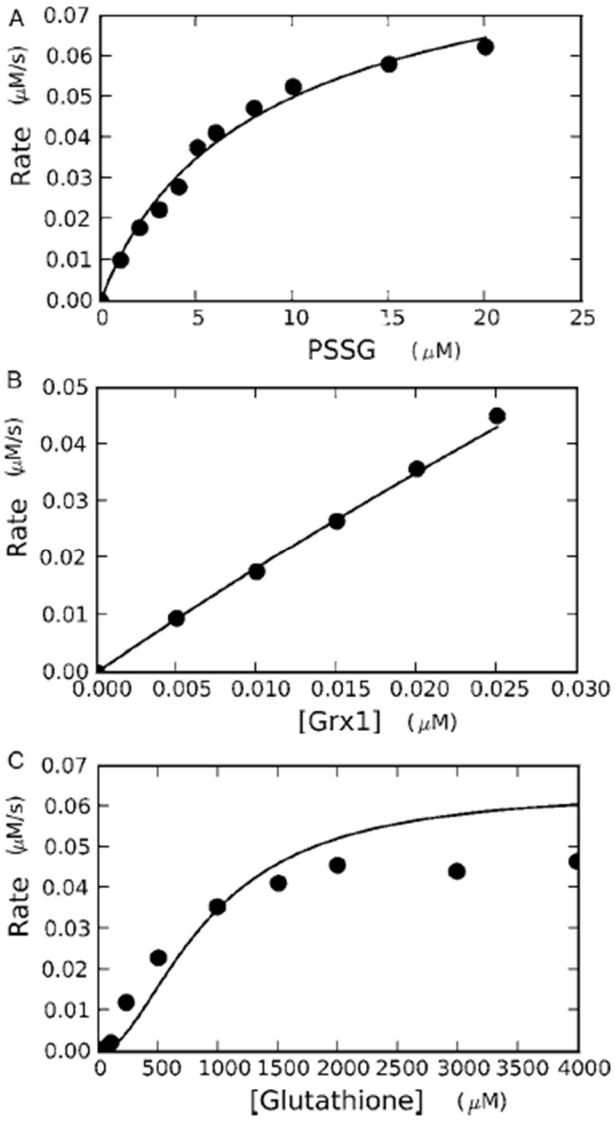

Figure 2.2: Comparison of kinetic model of glutaredoxin-dependent deglutathionylation of a protein disulfide (PSSG) (Scheme I) and an *in vitro* dataset. *(A)The kinetic model was fitted to an in vitro dataset for E. coli glutaredoxin kinetic activity. The kinetic model was able to predict the independent datasets for Grx1 (B) and glutathione (C) not used in the original fitting experiment (Pillay et al., 2009).*

The kinetic model used in Scheme I was based on the dithiol mechanism as opposed to the monothiol mechanism for deglutathionylation by glutaredoxins. The dithiol mechanism (Figure 2.3A), relies on both the N and C terminal cysteines of the glutaredoxin. The N-terminal cysteine of the reduced glutaredoxin reacts with the glutathionylated protein or PSSG, which leads to the formation of a mixed disulfide. The mixed disulfide reacts with the C-terminal cysteine, which separates the protein from the glutathione and leaves an

intramolecular disulfide glutaredoxin (GrxSS). In the last step of the dithiol reaction, GrxSS is reduced by two glutathione molecules (Figure 2.3A) (Holmgren et al., 2005). The monothiol mechanism, which was originally believed to be the true kinetic mechanism of deglutathionylation by glutaredoxins (Mieyal et al., 2008; Deponte, 2013; Lillig and Berndt, 2013; Mashamaite et al., 2015b), involves selective double displacement and only requires the N-terminal cysteine to react with the PSSG to form GrxSSGSH, which is reduced by glutathione (Mieyal et al., 2008). Interestingly, the dithiol reaction required two molecules of glutathione whilst the monothiol reaction appeared to require only one molecule. However, the monothiol mechanism also included a non-productive 'side-reaction' and once this reaction was taken into account, the two mechanisms were identical (Mieyal et al., 2008; Mashamaite et al., 2015b). Mashamaite *et al* (2015) also provided an explanation for the numerous other discrepancies between the dithiol and monothiol mechanisms. For example, the discrepancies in the double reciprocal patterns obtained for glutaredoxin activity was explained by the reversibility of deglutathionylation reaction for some substrates and not others (Mashamaite et al., 2015a).

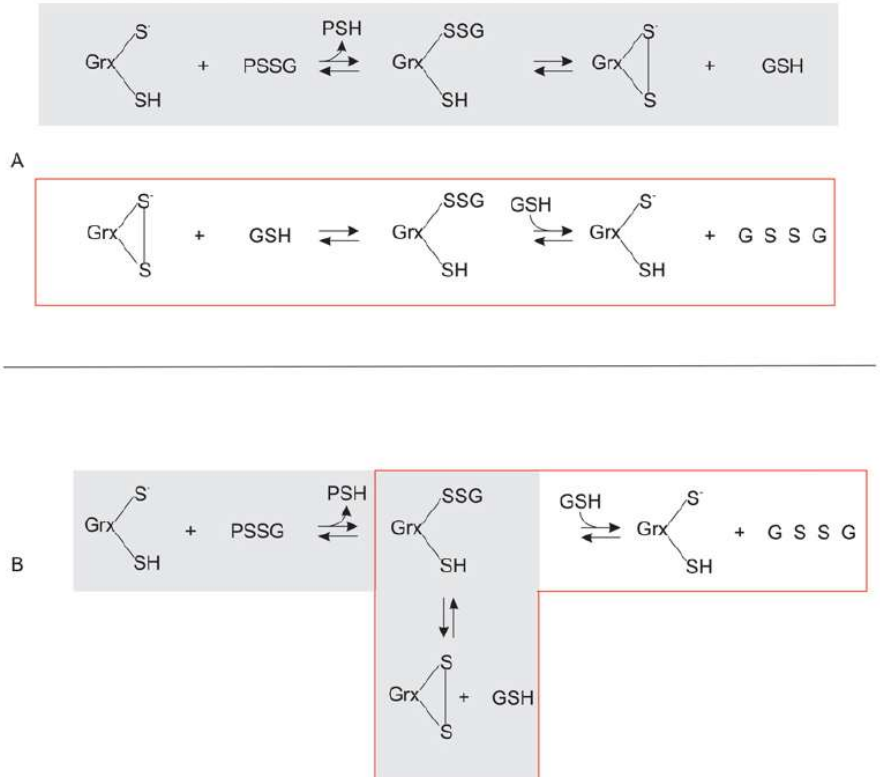

Figure 2.3: The two opposing mechanisms of glutaredoxin activity. *The dithiol mechanism (A) involves the formation of disulfide intermediate which was regarded as the product of a non-productive reaction in the monothiol mechanism (B). However, once this reaction was taken into account, both mechanisms were in fact identical. (Mashamaite et al., 2015)*

Subsequent to this paper, work by the Deponte group still continued to describe the monothiol ping-pong mechanism as the true mechanism of glutaredoxin activity which raised the question about the correctness of dithiol model (Begas et al., 2017; Deponte, 2017; Liedgens and Deponte, 2018). In order to resolve this, it was necessary to reassess the two competing models for glutaredoxin activity -the monothiol "ping-pong" (Reaction 4) and the dithiol (Scheme I) mechanisms (Cleland, 1963).

$$v = \frac{V_{max}}{\frac{k_x}{X} + \frac{k_y}{Y}} \tag{4}$$

In general terms, a ping-pong reaction is defined as a reaction with two substrates, a reaction intermediate (in this case, a covalently modified enzyme), two enzyme-substrate complexes and two products (Cleland, 1963; Srinivasan et al., 1997; Deponte, 2017). The ping-pong model for glutaredoxin activity advocates that the protein (substrate) becomes deglutathionylated and is released during the oxidative half-reaction and a glutaredoxin mixed disulfide is formed (Figure 2.4). Following this, glutaredoxin is reduced by free reduced glutathione (GSH) (Begas et al., 2015).

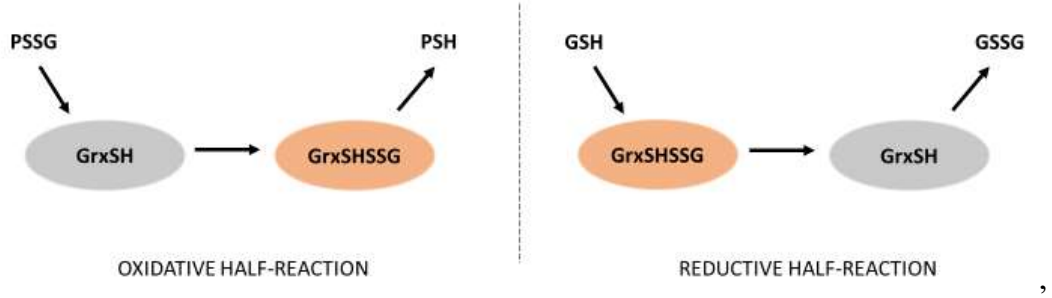

Figure 2.4: Ping-pong mechanism of deglutathionylation by glutaredoxin. *In the oxidative half-reaction, the glutathionylated peptide (PSSG) is reduced by reduced glutaredoxin (GrxSH), resulting in the formation of the mixed disulfide (GrxSHSSG). GrxSH is recovered in the reductive half-reaction by the addition of one molecule of GSH. Figure based on Srinivasan et al (1997), Begas et al (2015) & Deponte et al (2017).*

The side reaction which results in the formation of GrxSS is considered unnecessary in this model (Deponte, 2013). This mechanism requires a single GSH molecule and only the N-terminal cysteine residue of the glutaredoxin active site. However, the predictive value of this model has not yet been tested, so it is difficult to assess its validity. In addition, the ping-pong model does not provide an explanation for the high concentrations of GSH present in

the cell (Deponte, 2017). We therefore tested the validity of the ping-pong mechanism advocated by the Deponte group.

We also hypothesized that the seemingly futile side reaction which forms GrxSS (Figure 2.3), may have functional significance as glutaredoxins could be temporarily inactivated during oxidative stress conditions (low GSH concentration). If glutaredoxins were active during oxidative stress conditions, their activity could expose labile thiol residues to ROS. Thus, ROS-dependent decreases in GSH concentrations could trap glutaredoxins in their oxidized, inactive form (GrxSS, Figure 2.3). Once the GSH levels recovered, the glutaredoxins could be active and proteins would be deglutathionylated during the post-stress recovery period. Therefore, this hypothesis could provide an explanation for the side-reaction which was considered to be redundant by some authors (Gallogly et al., 2008; Mieyal et al., 2008; Deponte, 2013; Begas et al., 2017). In this chapter, computational modeling was used to test the hypothesis that glutaredoxin activity is regulated kinetically by the availability of GSH in the system.

2.2 Methods

Kinetic modeling was undertaken using Python Simulator for Cellular Systems (PySCeS) (http://pysces.sourceforge.net/) (Olivier et al., 2005). The models used were developed and validated previously by this group using published data (Pillay et al., 2009; Mashamaite et al., 2015a) and BRENDA database (available at: www.brenda-enzymes.org) (Jeske et al., 2018). Data points were taken from published figures using PlotDigitizer software (Huwaldt and Steinhorst, 2013).

2.3 Results

2.3.1 Systematic review of glutaredoxin datasets used for kinetics

In most studies of glutaredoxin activity, the parallel line pattern observed in double reciprocal plots which was presumed to be indicative of the ping-pong mechanism (Tsopanakis and Herries, 1975). However, both Pillay *et al* (2009) and Mashamaite *et al* (2015) showed that this ping-pong pattern is simply a structural feature of redox systems with two moiety conserved cycles. Therefore, testing the ping-pong model required fitting it to experimental datasets and assessing the fitted model's ability to predict independent datasets.

Datasets were sourced by searching on BRENDA database and literature. However, many of the published datasets had limitations for kinetic analyses and were not suitable for

comparison. Common defects amongst datasets were the limited number of data points used to determine kinetic parameters and missing information such as concentrations used in specified assays (Table 2.1). Moreover, the effect of GSH, which is a major predicted difference in the ping-pong and dithiol models for glutaredoxin activity, was usually not assessed in these assays.

Table 2.1: Examples of datasets unsuitable for fitting analysis

Organism	Problem	Reference
Plasmodium falciparum (Pf)	Only showed impact of [GSH] on *PfAOP** and not *PfGrx*	(Djuika et al., 2013)
S. cerevisiae	Only 3 data points used for kinetic analysis	(Discola et al., 2009)
S. cerevisiae	Assay only used monothiol glutaredoxins which would obviously use the monothiol mechanism	(Eckers et al., 2009)
E. coli	Only substrate used was arsenate	(Shi et al., 1999)
Homo sapiens	All enzyme concentrations used in assays were not described	(Gallogly et al., 2008)

**PfAOP* is *Plasmodium falciparum* Antioxidant Protein and *PfGrx* is *Plasmodium falciparum* glutaredoxin.

2.3.2 The ping-pong model cannot predict independent datasets

The validity of any kinetic model is based on two key factors – a) consistency with the dataset it is being fitted to and b) predictive ability of the fitted model. Peltoniemi *et al* (2006) performed *in vitro* assays using a homogeneous glutathionylated peptide (PSSG), GSH, glutathione reductase, *E. coli* Grx1 and NADPH to measure the deglutathionylation activity of glutaredoxins. Deglutathionylation activity was determined directly by measuring the formation of deglutathionylated substrate using fluorescence with excitation 280 nm and emission 356 nm (Peltoniemi et al., 2006). The ping-pong model (Equation 4) was fitted to datasets obtained from Peltoniemi *et al* (2006) using Python and the model was able to fit to the PSSG, GSH and Grx datasets individually (Figure 2.5 A-C).

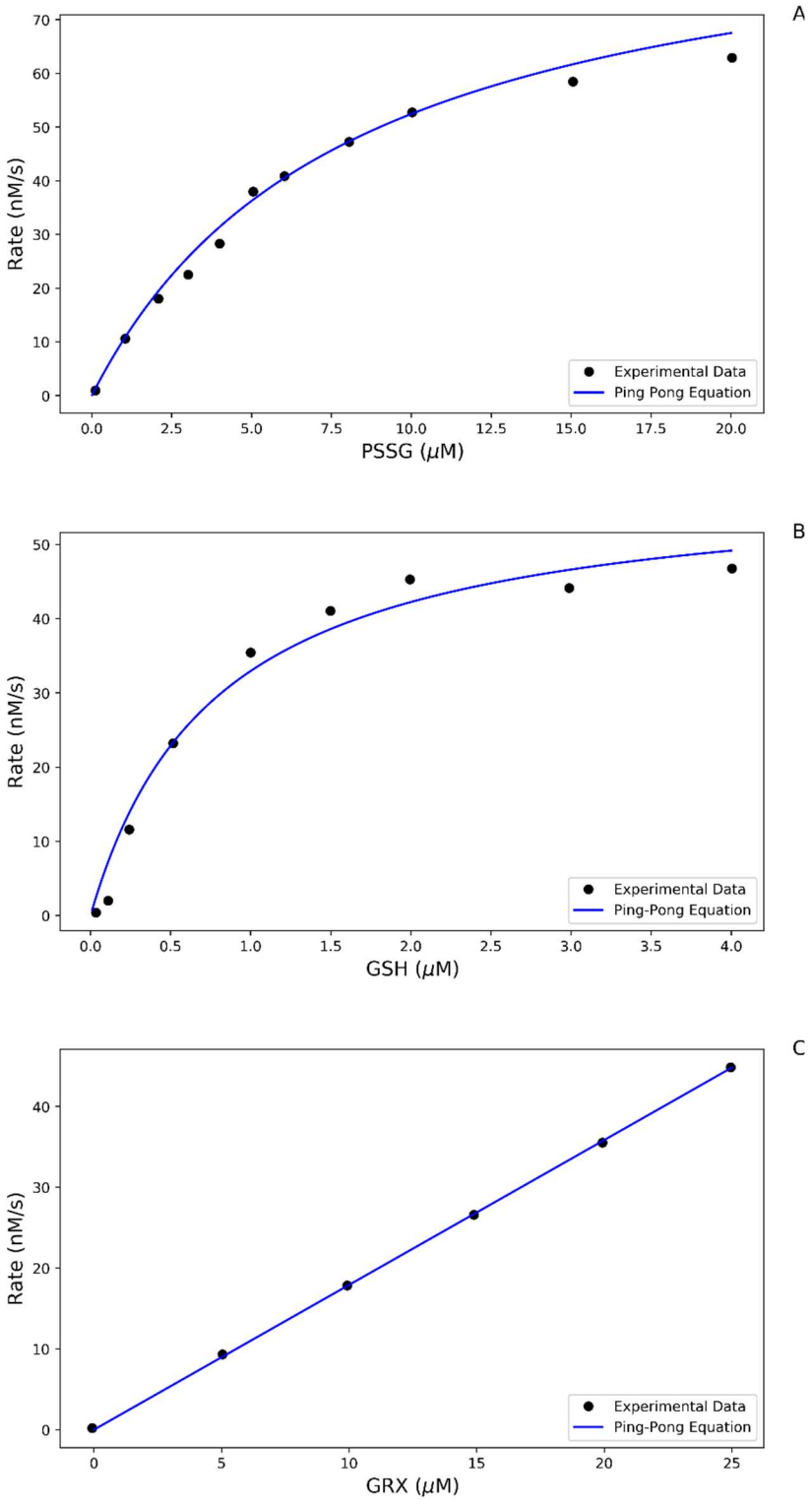

Figure 2.5: Data fitting using the ping-pong mechanism and data from Peltoniemi et al (2006). *The experimental data (●) was fitted to the ping-pong equation ((Vmax)/(1+(K_{PSSG}/PSSG)+(K_{GSH}/1000)), (solid line) for A) glutathionylated substrate (PSSG), B) GSH and C) GRX. The fitted parameters for these graphs are shown in Table 2.2.*

Table 2.2 Parameters obtained from fitting Peltoniemi *et al* (2006) dataset to the ping-pong equation

	Datasets		
Fitted parameters	**PSSG**	**GSH**	**Grx1**
k_{cat} (s^{-1})	4587.4	48108.85	*
K_{PSSG} (μM)	7.811	12.841	6.862×10^{-6}
K_{GSH}(μM)	31.876	15349.611	5.342×10^{-6}

*The enzyme concentration is changed in this dataset and therefore it is not possible to obtain a k_{cat} or V_{max}.

Using the Peltoniemi *et al* (2006) PSSG, glutaredoxin (Grx1) and GSH datasets to the ping-pong model led to vastly different parameters from the fitting experiment (Table 2.2). The binding of the substrates to glutaredoxin was assumed to be independent (Cleland, 1963; Djuika et al., 2013) and therefore the fit was not assessed by identifiability analysis. This was surprising because of the similar enzyme and substrate concentrations used for these assays and the fitted parameters for the Grx dataset were appreciably smaller than the other fits.

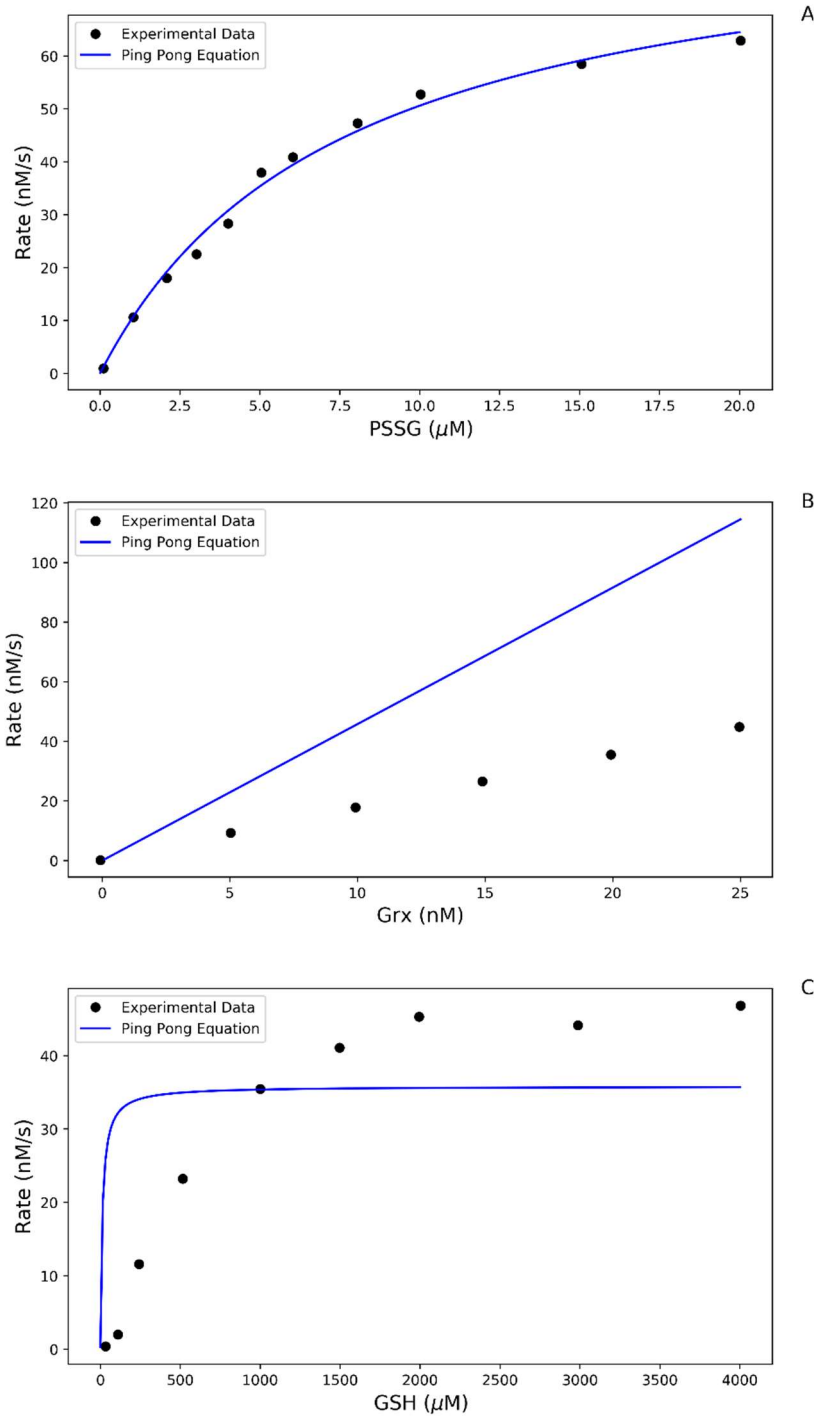

Figure 2.6 Prediction of Peltoniemi datasets using the ping-pong model. *The ping-ping model was fitted to the glutathionylated substrate (PSSG) dataset (A). The fitted parameters were used to predict independent datasets Grx (B) and GSH (C).*

Analogously to the modeling experiment undertaken for the dithiol model (Figure 2.2), the predictive value of the ping-pong model was tested. Using the parameters from fitting the ping-pong model to PSSG (Figure 2.5A, Figure 2.6A, Table 2.1), it was possible to determine whether or not the ping-pong model would be able to independently predict Grx

and GSH datasets. However, and as expected from the fitting results (Table 2.2), it was clear that the fitted ping-pong model failed to show any predictive value (Figure 2.6).

As the Peltoniemi *et al* (2006) dataset was an *E. coli* dataset, it could be argued that ping-pong model was only invalid for *E. coli* Grx1 and therefore we attempted to fit the ping-pong model to a yeast glutaredoxin dataset (Figure 2.7) (Li et al., 2010).

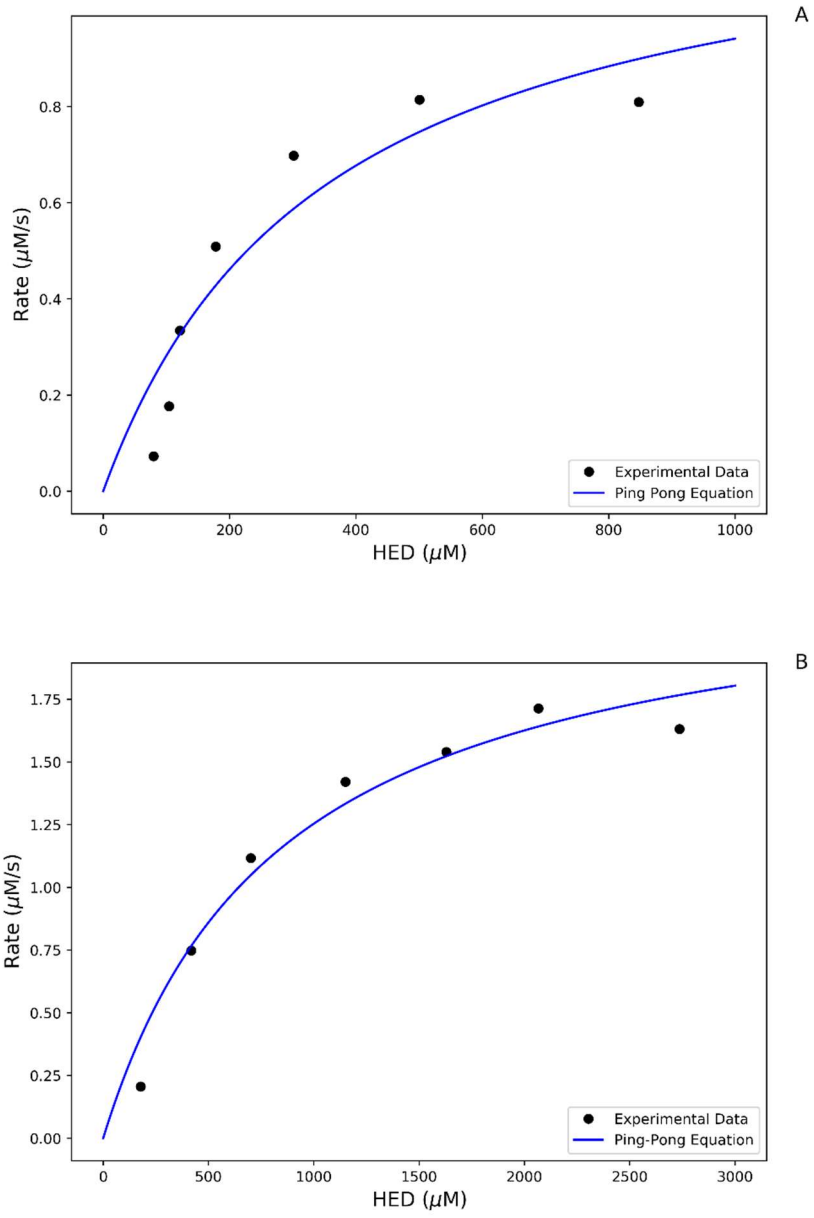

Figure 2.7 Data fitting using the ping-pong mechanism and data from Li et al (2010). *The experimental data (●) plotted against the ping-pong equation (solid line) for A yeast Grx1 (240 nM), HED vs Rate and B yeast Grx 2 (40 nM), HED vs Rate, with an enzyme. The fitted parameters for these graphs are included below (Table 2.3).*

While the ping-pong model could fit the yeast Grx1 and Grx2 datasets, fitted parameters obtained (Table 2.2) for the glutathione Michaelis constant values were not in the range of other published values for this parameter, in which K_{GSH} was 1.13 x 10^{-1} μM for Grx1 and 0.5μM for Grx2 (Li et al., 2010). The inconsistencies and lack of predictive power observed when the ping-pong model was tested with both the yeast and *E. coli* datasets showed that the previously validated dithiol model (Scheme I & Figure 2.2) was a better model of glutaredoxin/glutathione system.

Table 2.2 Parameters obtained from fitting Li *et al., 2010* dataset to ping-pong equation

Fitted parameters	Grx1	Grx2
k_{cat} (s^{-1})	0.005	0.023
K_{PSSG} (μM)	351.039	336.709
K_{GSH} (μM)	2.546 x10^{-6}	-0.600

2.3.3 Saturation of the redox cycles in the glutaredoxin/glutathione system

As a first step to testing the hypothesis of glutaredoxin inactivation, steady state simulations were performed on the glutaredoxin system, using the dithiol model, to understand the performance and regulation of this system. Substrate saturation is an inherent property of redox systems and occurs when the activity of the redoxin is limited by either its rate of reduction or oxidation (Pillay et al., 2009). Therefore, studying saturation cycles of redox cycles can give insight into the properties of the system. In order to do this, the oxidized and reduced inputs into the system were perturbed in our fitted *E. coli* model.

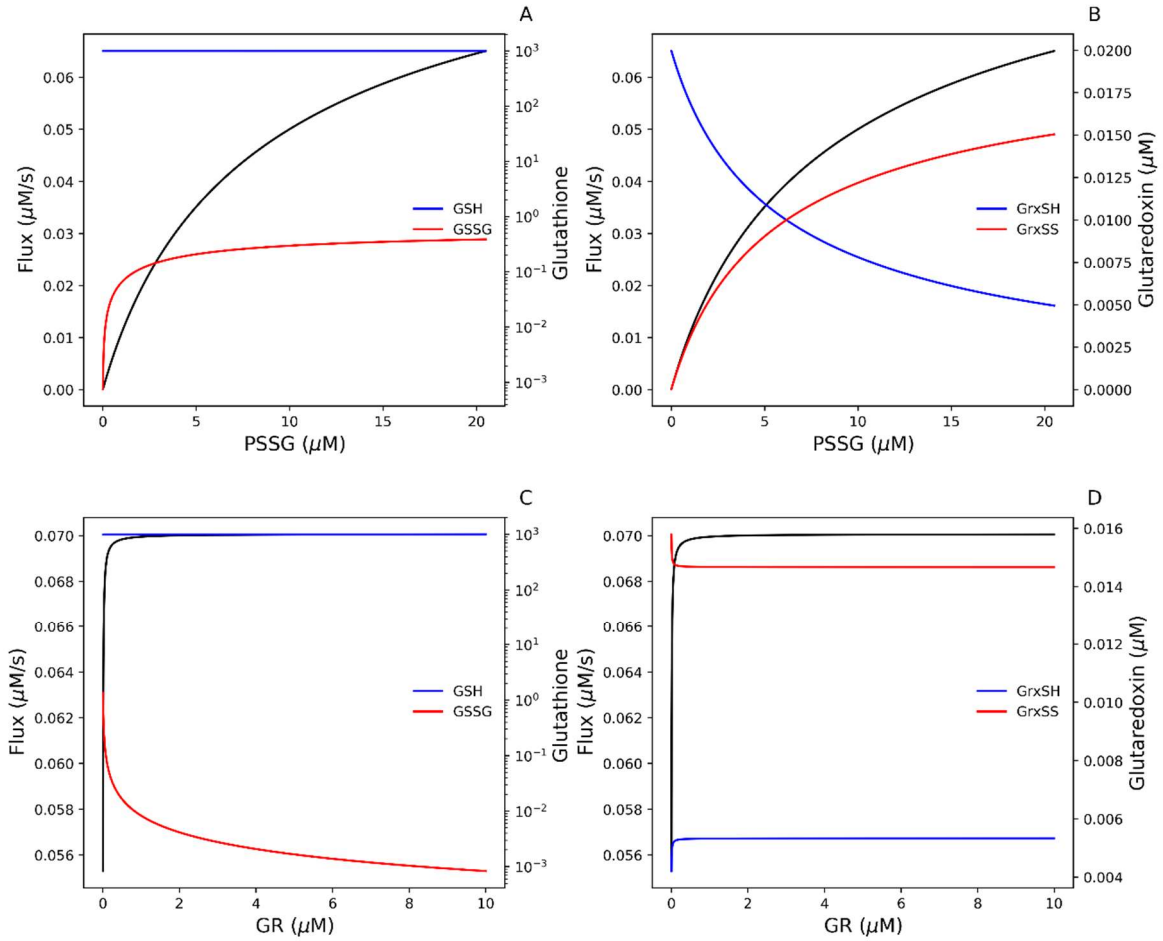

Figure 2.8: The effect of oxidative and reductive perturbations to glutathionylated protein and glutathione reductase on the flux and redox cycles in the glutaredoxin/glutathione system. *The effect of increasing the glutathionylated protein (PSSG) in the system on the glutathione (A) and glutaredoxin (B) redox cycles as well as the flux (black) was analyzed. Increasing the glutathione reductase (GR) increased the reduction of the glutathione (C) and glutaredoxin (D) redox cycles and the flux (black) was apparently saturated as the PSSG became limiting. Note that the GSH/GSSG couple was plotted in log space because of the high concentration of the glutathione moiety couple.*

As the glutathionylated protein substrate was increased, glutaredoxin distributed into its oxidized form and the flux reached an apparent maximum, which is observed when the flux reaches a plateau . Glutathione reductase is the enzyme responsible for reducing GSSG to GSH which in turn allows for the reduction of glutaredoxin to its reduced form (Scheme I, Figure 2.1). Thus, when glutathione reductase (GR) was increased, the active form of glutaredoxin (GrxSH) also increased (Figure 2.8D). Thus, this glutaredoxin model was

consistent with other computational models of redoxin systems, such as the *E. coli*, fission yeast, human cells and red blood cell models, with reductive perturbations associated with reduction of the redoxin moiety cycle and *vice versa* (Pillay et al., 2009; Adimora et al., 2010; Benfeitas et al., 2014; Tomalin et al., 2016)

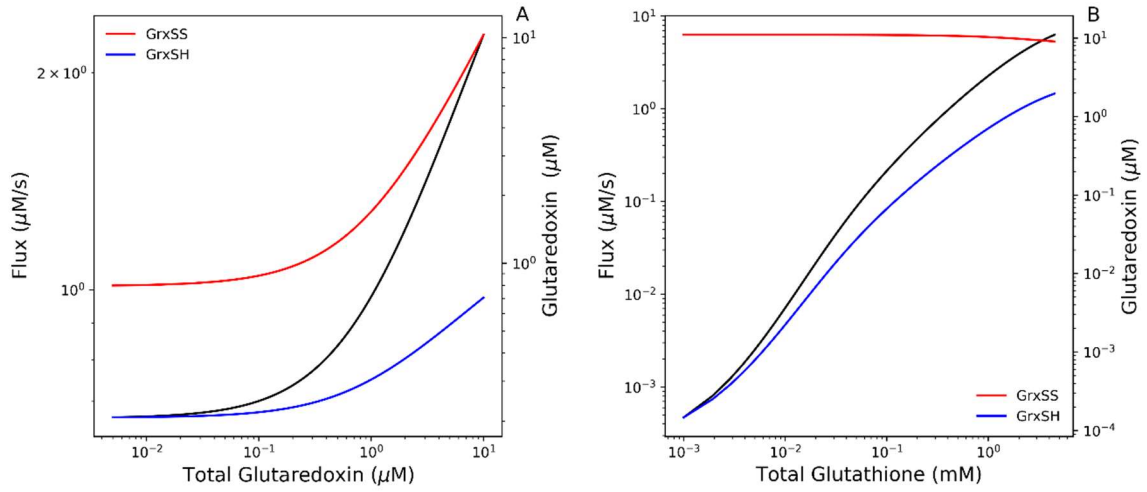

Figure 2.9: Saturating the redox cycles in the reduction of GrxSS by glutathione. *Increasing the total glutaredoxin (A) and glutathione (B) both resulted in increased active GrxSH. Reaction conditions: PSSG (5μM), GR (20nM) and NADPH (50μM).*

Glutathione is present at high intracellular concentrations but decreases during aging and other diseases (Table 1.1) and therefore the impact of total glutathione and total glutaredoxin perturbations were also analyzed (Figure 2.9). Increasing the total glutaredoxin in the system resulted in more than a fold-change increase in the activity of the deglutathionylation reaction. Consequently, this also resulted in an increase in the fraction of oxidized glutaredoxin (GrxSS) present in the system (Figure 2.9A). Increasing the total glutathione pool increased the flux and there was a negligible fold-change in the oxidized glutaredoxin (GrxSS) concentration in the system (Figure 2.9B, Supplementary Figure S2.1). This result contradicted our hypothesis that decreasing the total glutathione would result in a significant increase in GrxSS causing the system to be temporarily inactivated. However, it was interesting to note that an increase in GSH did result in an increase in the active glutaredoxin present in the system. In order to determine if changing these components could be relevant in regulating the system, the rate equation for Reaction 2 (Scheme I) was partitioned to determine the regulation of this system.

2.3.4 Flux partition reveals regulation of glutaredoxin by glutathione

The concentration of glutathione was shown to have a significant impact on the system (Figure 2.9B) which is significant as the reduction of glutaredoxin has been shown to be rate limiting in these systems (Srinivasan et al., 1997; Mashamaite et al., 2015a). This reaction (Reaction 2, Scheme I) was described by the following expression:

$$v = (k_2 \times GrxSS \times GSH^2)\left(1 - \left(\frac{\Gamma}{K_{eq2}}\right)\right) \quad (5)$$

$$\Gamma = \frac{\mathrm{GSSG} \times \mathrm{GrxSH}}{\mathrm{GrxSS} \times \mathrm{GSH}^2} \quad (6)$$

The first half of equation 5 (red), is the capacity term which represents the inherent reactivity of the two substrates, while the second half (blue) is the thermodynamic component of the reaction. For clarity, the mass action term is shown in equation 6. These components were partitioned in order to determine the contribution of these components to the flux in the system. When the rate expression was partitioned, it was found that the capacity term was almost identical to the overall flux showing that this component of the reaction was limiting (Figure 2.10). The capacity term consists of k_2 which is invariant at a given temperature and pressure, and oxidized glutaredoxin (GrxSS) which is determined by the rate of deglutathionylation. Note that the total concentration of glutaredoxin is an important parameter (Figure 2.9) but interestingly, there is no evidence of glutaredoxin upregulation during oxidative stress. Finally, the concentration of glutathione is also an important parameter and is present in high intracellular concentrations that appear to vary with age and oxidative stress. Collectively these results show that the overall deglutathionylation rate is sensitive to the available concentration of glutathione in the system (Figure 2.9 - 2.10).

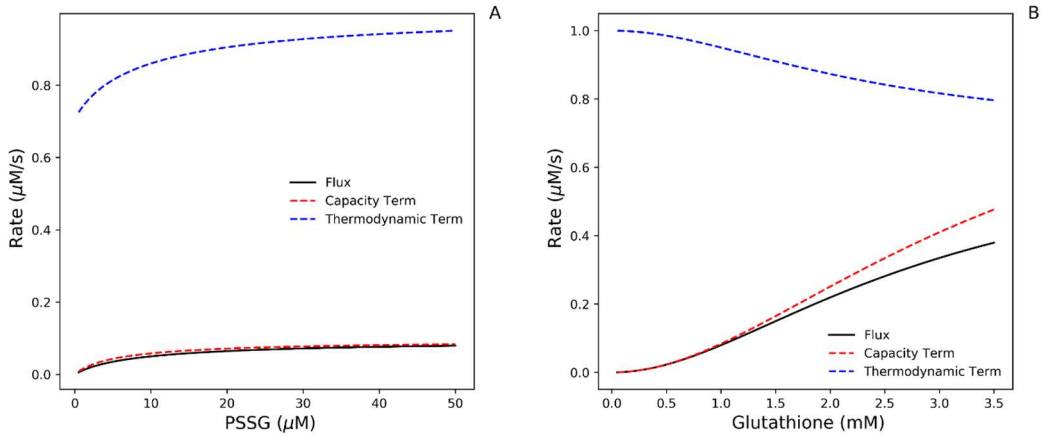

Figure 2.10: Determining the contribution of the capacity and thermodynamic components to the flux in the glutaredoxin/glutathione system. *The flux was partitioned into its capacity and thermodynamic components (equation 5) and plotted together with the flux (black). As PSSG was increased (A) the flux (black) was controlled by the capacity term (red), which is shown in red in equation 5. The same relationship was observed when the glutathione was increased (B).*

2.4 Discussion

Computational modeling provides a useful tool to explore the regulation of glutaredoxin systems but it was first necessary to assess the validity of the ping-pong and dithiol models proposed for these systems (Pillay et al., 2009; Deponte, 2013; Pillay et al., 2013; Mashamaite et al., 2015a). Unfortunately, finding suitable datasets to assess glutaredoxin datasets proved difficult as many published datasets were incomplete or included very few data points (Table 2.1). However, when using a high quality *E. coli* glutaredoxin dataset and a yeast glutaredoxin dataset (Peltoniemi et al., 2006; Pillay et al., 2009; Li et al., 2010; Mashamaite et al., 2015a) the widely accepted ping-pong model was found to be inadequate (Figure 2.2) and we therefore used the dithiol model for subsequent analyses.

Modeling of the glutaredoxin/glutathione system showed that the reduction of glutaredoxin disulfide by GSH is important in controlling the flux of the system and the overall GSH concentration may be responsible for the availability of active reduced glutaredoxin (Figure 2.10). Thus, loss of reduced glutathione would be expected to decrease glutaredoxin activity and the activity of the glutaredoxin system. Interestingly, a relationship between aging organisms and decline in GSH has been reported in literature (Sohal et al., 1990; Zhu et al., 2006). Based on these modeling results, a new hypothesis was formulated that the loss of glutathione associated with aging may reduce glutaredoxin activity and

increase the levels of glutathionylated protein which would impact cell function. To test this, *S. pombe* cells were aged to determine if there was indeed an age-related decline in GSH and an associated increase in protein glutathionylation levels.

Chapter 3: Investigating the relationship between chronological aging and glutathione concentration in *Schizosaccharomyces pombe*

3.1 Introduction

Despite the apparent abundance of GSH in cells, numerous studies have shown an age-associated decline in these levels, which was initially proposed to be a result of increased exposure to ROS with age (Sohal et al., 1990; Erden-İnal et al., 2002; Gil et al., 2006; Zhu et al., 2006). However, this has been disputed as based on its kinetics, GSH is not a major cellular antioxidant when compared to specialist ROS-scavengers such as peroxiredoxins and catalases (Deponte, 2013, 2017; Winterbourn, 2019). For example, the rate constant for the reduction of hydrogen peroxide by GSH is 0.8 $M^{-1}s^{-1}$ while the rate constant for equivalent reaction by peroxiredoxins is in the range of 10^6-10^8 $M^{-1}s^{-1}$ (Peskin et al., 2007; Giustarini et al., 2016). However, the high GSH levels may be necessary to support post-stress recovery processes such as deglutathionylation by glutaredoxins.

S. pombe or the fission yeast is considered a model organism for studying redox networks. First, it is often used to study the peroxiredoxin system due the presence of a single thiol peroxidase, Tpx1, making it more accessible than higher eukaryotes, while still providing insights that can later be translated to more complex organisms (Peskin et al., 2013b). Second, *S. pombe* cells can be readily cultured and analyzed when compared to higher eukaryotes (Hayles and Nurse, 2018) and there are detailed genomic and proteomic data available on *S. pombe* (Marguerat et al., 2012). Lastly, and most importantly for this research, *S. pombe* has only two cytosolic glutaredoxins and only one of these, Grx1, is a dithiol glutaredoxin. The other, Grx4 is a monothiol glutaredoxin that is primarily involved in iron-sulfur cluster formation ((Matsuyama et al., 2006). For these reasons, *S. pombe* was chosen as the organism in which to study the effects of aging on glutathione concentration.

Two types of aging can occur in yeast, namely replicative, which is determined by the number of replication scars present on the cells, and chronological aging which is, as the name suggests, aging that occurs over a period of days (Zuin et al., 2010). Chronological aging is most relevant in this case as it is the type of aging that is most relevant to higher eukaryotes including human cells. In the case of wild type *S. pombe*, chronological aging can be induced *in vivo* by simply inoculating a small volume of Edinburgh Minimal Media (EMM) with a single colony and incubating over a period of four to eight days without refreshing the media (Chen and Runge, 2009). This prevents the culture from continuing to replicate but allows the

cells to continue to survive and results in the exposure to higher levels of ROS as the media becomes depleted (Chen and Runge, 2009).

Following aging, GSH concentrations can be determined using the DTNB (5,5' dithiobis (2-nitrobenzoic acid) recycling assay (Tietze, 1969; Baker et al., 1990). DTNB reacts with GSH to produce 5-thionitrobenzoic acid, a yellow chromophore that can be measured spectrophotometrically at a wavelength of 415 nm (Baker et al., 1990). To the best of the author's knowledge, there is no published data on the relationship between aging and glutathione concentrations in fission yeast. Glutathionylation levels can be determined using the 2,3-naphthalenedicarboxaldehyde (NDA) assay which will measure the amount of GSH attached to proteins (Menon and Board, 2013). This assay relies on the reduction of the disulfide bonds between proteins and glutathione by dithiothreitol (DTT), which subsequently releases the GSH. The GSH is then free to react with NDA to form a highly fluorescent product (Orwar et al., 1995). Determining the levels of protein glutathionylation in the young and aged cultures was expected to provide a baseline to investigate the effect of a decrease or increase in glutathione on cell recovery. In addition to aging, L-buthionine- (S, R)-sulfoximine (BSO) has also been shown to deplete glutathione levels. BSO inhibits the synthesis of glutathione by inhibiting the activity of γ-glutamylcysteine-synthetase (Ghezzi, 2013). There is currently no published data showing the relationship between age and glutathione concentration in *S. pombe* and therefore these parameters will be compared with the decline in glutathione that is associated with BSO. We note that the data presented in this chapter represents exploratory research and as such needs to be further verified.

3.2 Materials

The wildtype *S. pombe* 972 (h-) strain used in this project was kindly provided by Dr. Elizabeth Veal (Newcastle University, UK) (Bozonet et al., 2005). Glutathione reductase, 2,3 naphthalenedicarboxaldehyde, reduced glutathione, L-buthionine- (S, R)-sulfoximine and 5,5' dithiobis 2-nitrobenzoic acid were purchased from Sigma Aldrich (Germany). Dithiothreitol was purchased from Capital Labs (South Africa) and the Pierce™ BCA™ Assay Kit was purchased from Thermofisher (USA)

3.3 Preparation of culture media

3.3.1 Yeast extract (YE) media

YE plates were prepared by combining yeast extract (0.5%), glucose (2%) and agar (2%).

3.3.2 Edinburgh minimal media (EMM)

EMM was prepared by combining potassium hydrogen phthalate (14.7 mM), di-sodium hydrogen orthophosphate (15.5 mM), ammonium chloride (93.5 mM), glucose (2%) with salt stock (1 X), vitamin stock (1 X) and mineral stock (1 X) into dH_2O. The media was autoclaved at 120°C for 15 minutes (Hayles and Nurse, 2018).

3.4 Preparation of reagents & buffers

3.4.1 Salt stock (50 X)

Salt stock was prepared by combining magnesium chloride (260 mM), calcium chloride (4.99 mM), potassium chloride (670 mM), di-sodium sulphate (14.1 mM) into dH_2O.

3.4.2 Vitamin stock (1000 X)

Vitamin stock was prepared by combining nicotinic acid (4.2 mM), myo-inositol (56 µM), biotin (40.8 µM), pantothenic acid (81.2 mM) into dH_2O.

3.4.3 Mineral stock (1000 X)

Mineral stock was prepared by combining boric acid (80.9 mM), manganese sulphate (23.7 mM), zinc sulphate (13.9 mM), ferric chloride (7.4 mM), molybdic acid (2.47 mM), potassium iodide (6.02 mM), copper sulphate (1.6 mM), citric acid (47.6 mM) into dH_2O.

3.4.4 Tris-HCl

0.5 M Tris-HCl was prepared by dissolving Tris and 0.1% Triton X-100 in dH_2O and corrected to pH 8 with HCl.

3.4.5 Glutathione quantification buffer

Glutathione (GSH) quantification buffer was prepared by dissolving EDTA (1 mM) and $Na_2PO_4.2H_2O$ (100 mM) in distilled water and the pH was adjusted to pH 7.5.

3.4.6 2,3 Naphthalenedicarboxaldehyde (NDA) derivation mix

The NDA derivation mix was prepared by combining 1 mL NDA in dimethyl sulfoxide (10 mM) with 7 mL Tris (50 mM, pH 10) and 1 mL sodium hydroxide (0.5 M).

3.5 Methods

3.5.1 Maintenance and cultivation of *Schizosaccharomyces pombe*

The strain used in this study, *S. pombe* wild-type 972 (h-) were revived from frozen stocks on YE agar for 3 days at 30°C, grown up in YE broth at 30°C for 2 days before being stored at -80°C in 50% (v/v) glycerol.

3.5.2 Growth and aging of S. pombe

Single colonies from the YE agar plates were used to inoculate 30 mL EMM to an initial OD_{600}~0.1. The cultures were grown for 5 days, using a previously described chronological aging protocol in an MRC Laboratory Shaker Incubator (30°C, 200 rpm shaking) (Chen and Runge, 2009), with or without the addition of GSH (1 mM) or BSO (1 mM). At 2 and 5 days, 2 mL of culture was harvested into 15 mL Falcon tubes on ice. Cells were pelleted by centrifugation (5000 x *g*, 5 minutes, 4°C) and stored at -80°C.

3.5.3 Preparation of cell supernatant and protein Samples

Pellets were thawed on ice and resuspended in 10% (w/v) TCA (200 µL). Solutions were transferred to 2 mL Ribolyser tubes to which 0.5 mm glass beads (750 µL) were added. Samples were placed in a bead beater for 15 seconds, transferred to ice for 1 minute and returned to the bead beater for a further 15 seconds. While on ice, 10 % (w/v) TCA (500 µL) was added to the tubes which were then pierced with a hot needle, to elute the protein, before being placed in a 1 mL Eppendorf tube inside a 50 mL Falcon tube. Samples were centrifuged (2000 x *g*, 1 minute, 20°C) to elute the sample out of the beads (Day et al., 2012). The Eppendorf tubes containing the samples were centrifuged (13000 x *g*, 10 minutes, 4°C) and the supernatant was transferred to Eppendorf tubes to be used for Glutathione recycling assay (Section 3.5.4). Protein pellets were washed in 100% acetone (200 µL) three times and air dried until pellets were white, resuspended in 0.5 M Tris-HCL buffer (40 µL) and incubated for 10 minutes at room temperature. DTT (final concentration 5 mM) was added to the protein solution to break the protein-disulfide bonds and elute the protein-bound GSH (30 minutes, room temperature). Protein was precipitated by addition of 25 µL 200 mM TCA and incubated for 30 minutes on ice. Samples were then centrifuged (20 000 x *g*, 20 minutes) and

supernatant was transferred to a clean tube to be used for the glutathionylation assay (3.4.5) (Menon and Board, 2013). Protein pellets were used to determine protein concentration using a Pierce™ BCA™ Assay Kit (Thermofisher, South Africa).

3.5.4 Glutathione recycling assay

GSH quantification was performed according to the method developed by Baker *et al* (1999). Briefly, 20 µL of cell supernatant was added to a 96-well microtiter plate, placed into a VersaMax™ ELISA Microplate Reader. The reaction mix was freshly prepared by adding DTNB (0.15 mM), NADPH (0.2 mM) and GR (1 U/mL) to 5.85 mL GSH quantification buffer containing EDTA 1mM and $Na_2PO_4.2H_2O$ (100 mM). The reaction mix was added to the 96-well plate containing the cell lysate immediately before the absorbance was read at 405nm for 2 minutes. GSH standards, used to develop a standard curve, were prepared by dissolving 1 mM GSH in water before diluting in GSH quantification buffer. The GSH concentrations of samples were determined by interpolation from a GSH standard curve.

3.5.5 Glutathionylation assay

The concentration of glutathione attached to proteins was determined by the NDA derivation method of Menon and Board (2013), in which 180 µL NDA derivation mix was added to 20 µL supernatant and standards in a 96 well plate. The plate was incubated in the dark (30 minutes, room temperature) and fluorescence was determined at 485 nm excitation and 520 nm emission respectively using an Optima FLUOstar fluorescence plate reader. A standard curve was created using the fluorescence of the GSH standards.

3.5.6 Statistical analysis

Tests of statistical significance were performed using the paired *t*-test with 95% confidence level using Python SciPy.

3.6 Results

3.6.1 Optical density readings determine that cultures survive five-day aging

As cultures were grown for a period of 5 days without refreshing the media in order to induce chronological aging and prevent continued replication, it was necessary to perform optical density readings after 2 and 5 days of incubation to confirm that the *S. pombe* 972 strain was able to survive five days without the addition of fresh media. There was a non-significant increase in the optical density of the *S. pombe* cultures between 2 and 5 days under all growth conditions, showing that the cells continued to survive without refreshing the media

(Figure 3.1). This was expected as Chen and Runge (2009) had shown that this method did not lead to a loss of cell viability. The cultures grown in media supplemented with either GSH or BSO had lower optical densities than the cultures grown in standard media after 2 days of growth, at 2.09, 1.56 and 1.45 respectively (Figure 3.1, Supplementary Table S3.1). Interestingly, there was a significant decrease in the growth observed in media with GSH as well as media with BSO when compared with EMM with no additions after 2 days (Table 3.1). However, as the OD_{600} increased in both *S. pombe* cultures grown with added GSH and BSO between 2 and 5 days, it can be concluded that the addition of glutathione or BSO was not lethal to the *S. pombe* cultures (Table 3.1).

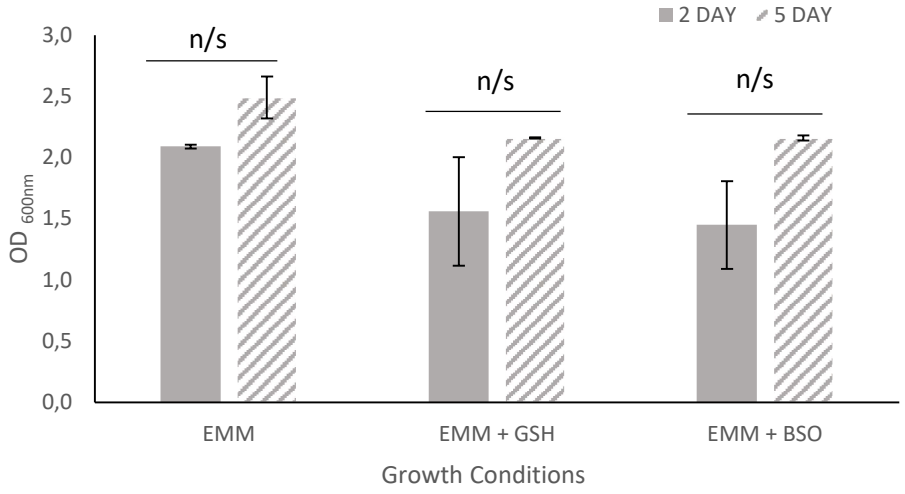

Figure 3.1: Optical density at 600 nm of *S. pombe* cultures grown under different conditions. *S. pombe grown in Edinburgh minimal media (EMM), EMM + 1 mM glutathione (GSH) and EMM + 1 mM L-buthionine- (S, R)-sulfoximine (BSO) all had an increase in OD600 readings. Significance denoted as * $p < 0.05$ and n/s is not significant. (n = 6, standard error shown in figure).*

Table 3.1 Paired *t*-test significance (p>0.05) between OD_{600} of *S. pombe* cultures in different growth conditions

Growth Conditions	2 Day		5 Day	
	Mean OD_{600}	Significance (p<0.05)	Mean OD_{600}	Significance (p<0.05)
EMM vs EMM + GSH	2.09 vs 1.56	Not significant (p= 0.054)	2.488 vs 2.16	Significant (p=0.0191)
EMM vs EMM + BSO	2.09 vs 1.65	Significant (p=0.0191)	2.488 vs 2.16	Not Significant (p=0.054)
EMM + GSH vs EMM + BSO	1.56 vs 1.65	Not significant (p=0.054)	2.16 vs 2.16	Not significant (p=0.89)

3.6.2 Aged *S. pombe* 972 cells showed an increase in free GSH

Reduced glutathione, ranging in concentration from 0 µM to 325 µM, was used to create a standard curve from which a linear regression was performed. GSH reaction buffer without GSH or sample was used as a negative control and showed no change when DNTB was added (Table S3.2, Supplementary Information).

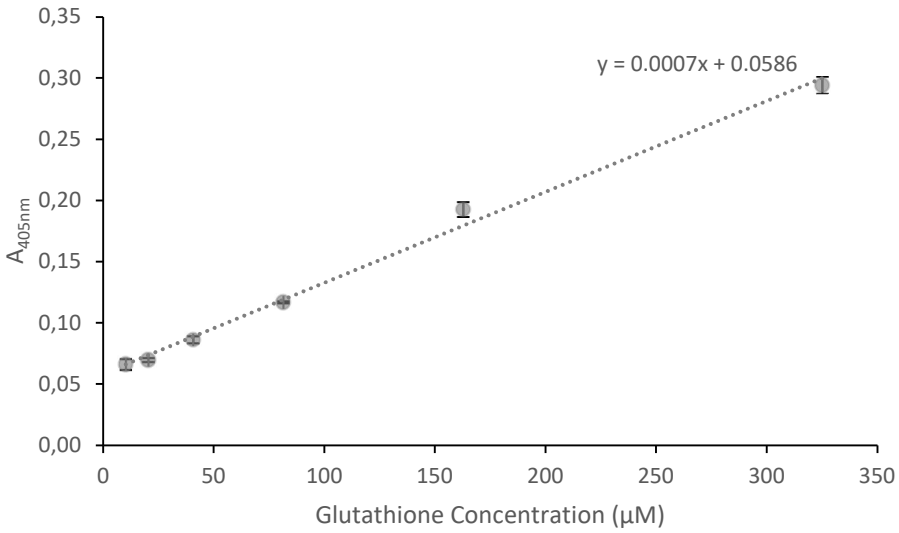

Figure 3.2: Glutathione recycling assay of known glutathione concentrations. *A standard curve was created from the absorbance at 405 nm of glutathione ranging in concentration between 10.2 µM and 325 µM. The linear trend line had an r^2 value= 0.994. (n =3, standard errors shown in figure)*

The linear equation from Figure 3.2 was used to determine the free GSH concentration of the *S. pombe* cell supernatants (Section 3.5.3) subjected to the DNTB glutathione recycling assay (Section 3.5.4). Glutathione concentrations were then corrected for growth by dividing the average of the six glutathione concentrations obtained for each growth condition by the average OD_{600} (Supplementary Table S3.1; S3.2).

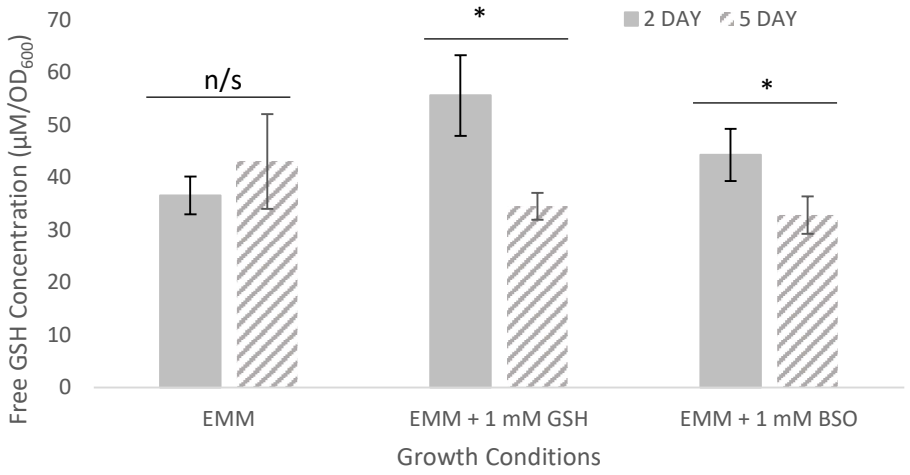

Figure 3.3 Concentration of free glutathione from *S. pombe* grown in different media. *Free cellular glutathione concentrations of S. pombe grown in Edinburgh minimal media (EMM), EMM + 1 mM glutathione (GSH) and EMM + 1 mM L-buthionine- (S, R)-sulfoximine (BSO) were measured by fluorescence in the glutathione recycling assay by Baker et al (1999) and corrected for the OD600 of the respective cultures (Section 3.54). Significance denoted as * $p < 0.05$ and n/s is not significant. (n=6, standard errors shown in figure)*

GSH concentrations were corrected to take into account the increase in optical density that occurred with growth as it is assumed that an increase in cell number would increase GSH concentration (Table S3.1). As expected, there was a significant increase in free glutathione in *S. pombe* grown for 2 days in EMM supplemented with GSH when compared with the *S. pombe* grown in EMM with no supplementation (Table 3.2). There was also a significant difference in the free glutathione for those cultures that included BSO. In the 5-day aged cultures under normal growth conditions (EMM), the free cellular glutathione concentration significantly increased from 36.62 µM to 43.09 µM. By contrast, there was a significant decrease in the free GSH levels in those cells that were treated with BSO. A comparison of

the 5-day old cultures showed that the different treatments yielded significantly different levels of free GSH (Table 3.2). Collectively, these results showed that the addition of GSH had a significant effect on the free glutathione levels within cells and BSO decreased these levels in aged cells. Cells without supplementation showed an increase in GSH levels that was not determined to be significant. We next aimed to determine the effect of these treatments on protein glutathionylation levels.

Table 3.2 Paired *t*-test significance ($p<0.05$) between free glutathione concentrations of *S. pombe* cultures in different growth conditions

	2 Day		5 Day	
Growth Conditions	Mean GSH (μM)	Significance ($p<0.05$)	Mean GSH (μM)	Significance ($p<0.05$)
EMM vs EMM + GSH	36.62 vs 55.67	Significant ($p=0.007$)	43.09 vs 34.55	Significant ($p=0.043$)
EMM vs EMM + BSO	36.62 vs 44.34	Not significant ($p=0.087$)	43.09 vs 32.86	Significant ($p=0.023$)
EMM + GSH vs EMM + BSO	55.67 vs 44.34	Not significant ($p=0.116$)	34.55 vs 32.86	Not Significant ($p=0.440$)

3.6.3 Protein glutathionylation of *S. pombe* decreases with age

As previously discussed, aging is often linked with increased exposure to ROS and as a result glutathionylation is expected to increase. Glutathionylation levels were tested indirectly by isolating *S. pombe* total protein and chemically cleaving glutathione from proteins. The protein was then removed to prevent any interaction with the assay, and the remaining glutathione concentrations were determined using the NDA fluorescence assay. These data were normalized for changes in protein concentration which were expected to occur as the cultures aged. Protein concentrations were determined using the BCA assay (Figure 3.4 and 3.5).

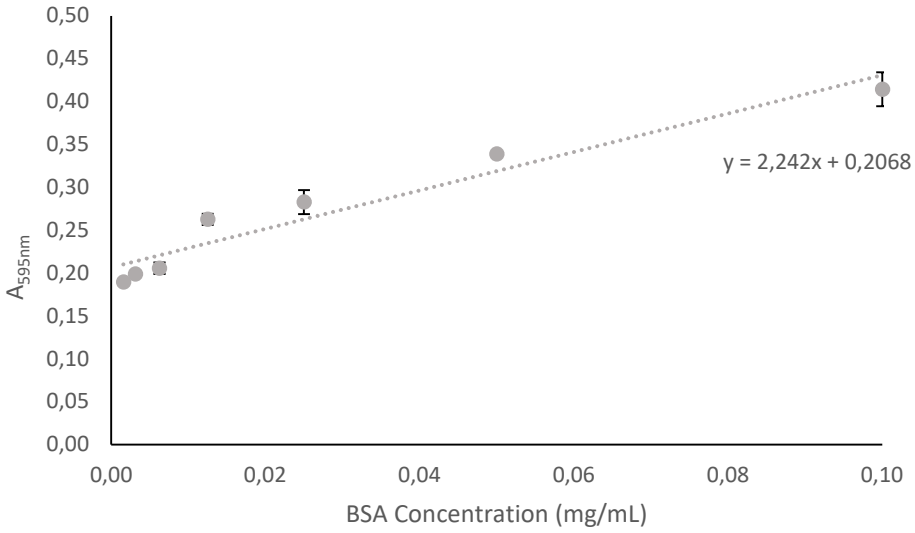

Figure 3.4: BCA assay of known protein concentrations. *A standard curve was created from the absorbance at 595 nm (A_{595}) of known concentrations of bovine serum albumin (BSA) (ranging from 0.0015 mg/mL to 1 mg/mL) obtained during the BCA assay. The linear trend line had an r^2= 0.9341. The linear equation was used to determine the protein concentration of the samples (n=3, standard errors shown in figure).*

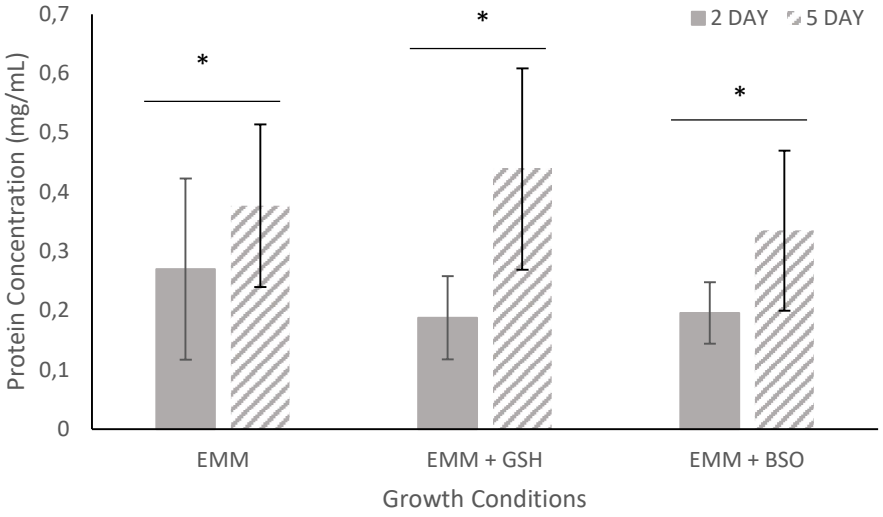

Figure 3.5: Protein concentrations of *S. pombe* cultures grown in different media. *Protein concentrations were determined using the fluorimetric BCA assay. (Section 3.5.3). The protein concentration of S. pombe cultures grown in Edinburgh minimal media (EMM), EMM + 1 mM glutathione (GSH) and EMM + 1 mM L-buthionine- (S, R)-sulfoximine (BSO) were compared for 2- and 5-days of growth. Significance denoted as * $p < 0.05$ and n/s is not significant, (n=6, standard errors shown in figure).*

Between 2 and 5 days, protein concentrations significantly increased in *S. pombe* grown in standard EMM (from 0.27 mg/mL to 0.377 mg/mL) and EMM with additional GSH (0.188 mg/mL to 0.439 mg/mL) or 1 mM BSO (0.196 mg/mL to 0.335 mg/mL), confirming that cultures continued to grow over the aging period. Cleaved glutathione concentrations obtained in the NDA assay (Figure 3.6) were corrected for protein concentrations obtained in the BCA assay by dividing the glutathione concentrations by the relevant protein concentration. Figure 3.7 shows the relative glutathione concentration (µM) cleaved per mg/mL of *S. pombe.*

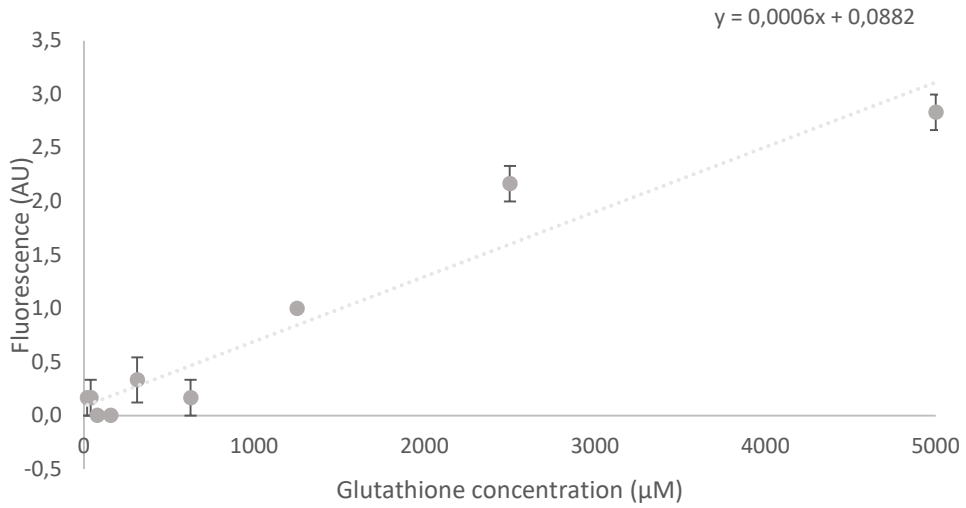

Figure 3.6: Naphthalenedicarboxaldehyde assay of known glutathione concentration. *A standard curve was created from known concentrations of glutathione (µM) and the fluorescence readings (AU) obtained during the Naphthalenedicarboxaldehyde* **(***NDA) assay. The linear trendline had an* r^2 *= 0.9341.(n=3, standard errors shown in figure).*

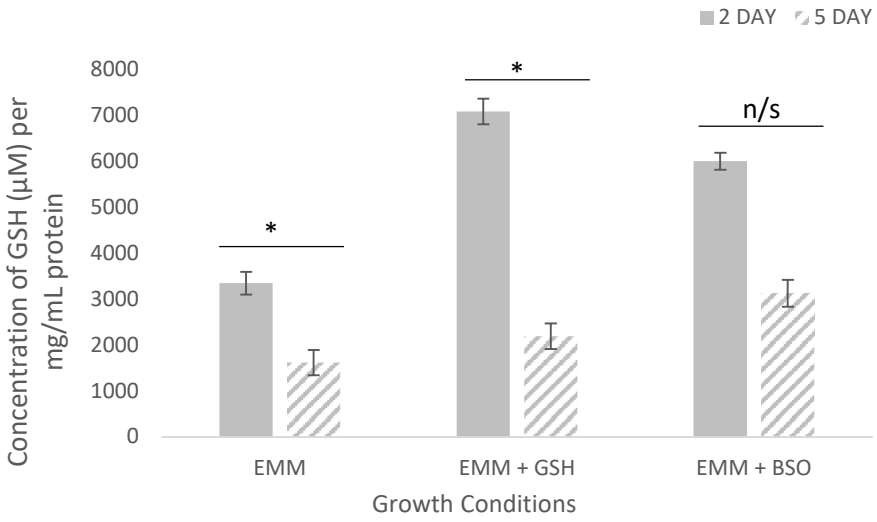

Figure 3.7 Protein glutathionylation levels per mg/mL of protein in *S. pombe* grown in media with different additives. *The concentration of cleaved glutathione obtained in the NDA assay of S. pombe grown in Edinburgh minimal media (EMM), EMM + 1 mM glutathione (GSH) and EMM + 1 mM L-buthionine- (S, R)-sulfoximine (BSO) was divided by the protein concentration to show the amount of glutathione present per mg/mL of protein. Significance was denoted as * $p < 0.05$ and n/s is not significant. (n=6, standard errors shown in figure)*

In contrast to our hypothesis, the NDA assay showed that the glutathionylation levels decreased in all growth conditions between 2- and 5-day growth periods. Glutathionylation levels decreased significantly in *S. pombe* grown in EMM and in EMM with 1 mM added glutathione, but the decrease in glutathionylation levels in *S. pombe* grown in EMM with 1 mM BSO was not significant (Figure 3.7, Supplementary Data Table S3.5). When comparing the treatments, the increase in glutathionylation levels between *S. pombe* grown in EMM for 2 days and in EMM with GSH for 2 days and in EMM with 1 mM BSO for 5 days was significant. All other treatments showed no significant changes.

Table 3.3 Paired *t*-test significance ($p<0.05$) between protein glutathionylation levels of *S. pombe* cultures in different growth conditions

Growth Conditions	2 Day		5 Day	
	Mean glutathionylation (μM per mg/mL)	Significance ($p<0.05$)	Mean glutathionylation (μM per mg/mL)	Significance ($p<0.05$)
EMM vs EMM + GSH	1890.04 vs 1332.26	Significant ($p=0.033$)	1519.67 vs 962.98	Not significant ($p=0.48$)
EMM vs EMM + BSO	1890.04 vs 1177.11	Not significant ($p=0.213$)	1519.67 vs 1047.46	Significant ($p=0.03$)
EMM + GSH vs EMM + BSO	1332.26 vs 1177.11	Not significant ($p=0.057$)	962.98 vs 1047.46	Not significant ($p=0.84$)

3.7 Discussion

An age-associated decline in glutathione concentrations has previously been shown in a number of organisms, such as rats, fruit flies and humans (Sohal et al., 1990; Erden-İnal et al., 2002; Gil et al., 2006; Zhu et al., 2006) but, to our knowledge, no data is available on the effect of aging on the glutathione concentration in *S. pombe*. Before the cause of age associated GSH decline could be elucidated, it was necessary to determine if this decline is present in *S. pombe*. Two-day old *S. pombe* (strain 972) cultures were compared with aged cultures (five-day old). Factors considered were the free glutathione concentrations and glutathionylation levels.

The relationship between GSH concentration and age was tested in chronologically aged *S. pombe* cultures by growing cultures without refreshing the limited volume of minimal media for a period of five days (Chen and Runge, 2009). Optical density readings showed that the yeast cultures did survive the five-day period, but it was not possible to be sure that the cultures had in fact aged. Future research into confirming this would be beneficial as it is possible that cultures might require a longer period of aging.

The method for testing glutathione concentrations was proposed by Tietze and has been adapted for use in microtiter plates which is an improvement as it requires smaller volumes of sample than the traditional method (Baker et al., 1990). The assay was repeated

six times using six replicates for each treatment and in each repeat, the same pattern of increasing glutathione was observed. Interestingly, the expected age-associated decline in glutathione was not observed in *S. pombe* cells grown in standard EMM. Unexpectedly, we found that free glutathione concentrations *increased* between the two- and five-day aged *S. pombe* cells grown in EMM (Figure 3.3). The addition of 1 mM of GSH to the EMM resulted in a significant increase in free glutathione when compared with that of cells grown in EMM for 2 days. However, free glutathione levels declined between 2 and 5 days in the cultures grown with additional GSH which was also not expected. As expected, the cultures grown in the presence of GSH synthesis inhibitor BSO showed a significant decline in cellular GSH concentrations, it is not clear why this is not the case when compared to cultures grown in EMM alone.

Aged cells were expected to have higher levels of protein glutathionylation due to increased exposure to ROS (Di Stefano et al., 2006). The NDA assay for glutathionylation showed that the concentrations of GSH cleaved from glutathionylated proteins also increased as cultures were aged. However, as glutathionylation occurs when glutathione becomes attached to vulnerable cysteine residues in proteins, it was necessary to consider that the cell growth and replication that occurred between the two and five day sampling was likely to have increased the culture protein concentration and consequently the amount of protein which could be glutathionylated (Mieyal et al., 2008; Ghezzi, 2013). Therefore, protein concentrations were determined and found to increase with age as was expected. The glutathione concentrations obtained in the glutathionylation assay were subsequently corrected against these concentrations. These data showed that the glutathionylation levels were in fact decreased as the cells aged, in all growth conditions, including in the presence of GSH synthesis inhibitor, BSO (Figure 3.7). We expected that glutathionylation levels would decrease when *S. pombe* cells were grown in EMM supplemented with GSH if it is the limiting factor in the glutaredoxin/glutathione system. However, the significant decrease in protein glutathionylation in the EMM (Figure 3.7 A) and the similar glutathionylation levels in aged BSO-treated cultures were surprising. We speculate that in the EMM cultures, compensatory GSH synthesis may have activated the glutaredoxin system (Figure 3.8). The rate-limiting enzyme in the glutathione biosynthesis pathway, γ-glutamylcysteine-synthetase, is negatively regulated by the glutathione levels in the cell. In the EMM cells, aging would have induced an increase GSH biosynthesis which would have increased the free glutathione levels (Figure 3.3) resulting in a decrease in protein glutathionylation (Figures 3.7, 3.8). In cells supplemented with GSH, the glutathione biosynthesis pathway would be repressed therefore

there was no change in free glutathione levels in these cells (Figure 3.7). The decreased levels of deglutathionylation in the cells could come from either increased glutaredoxin activity or a reduction in protein glutathionylation (Figure 3.8). Unfortunately, we were unable to test these options.

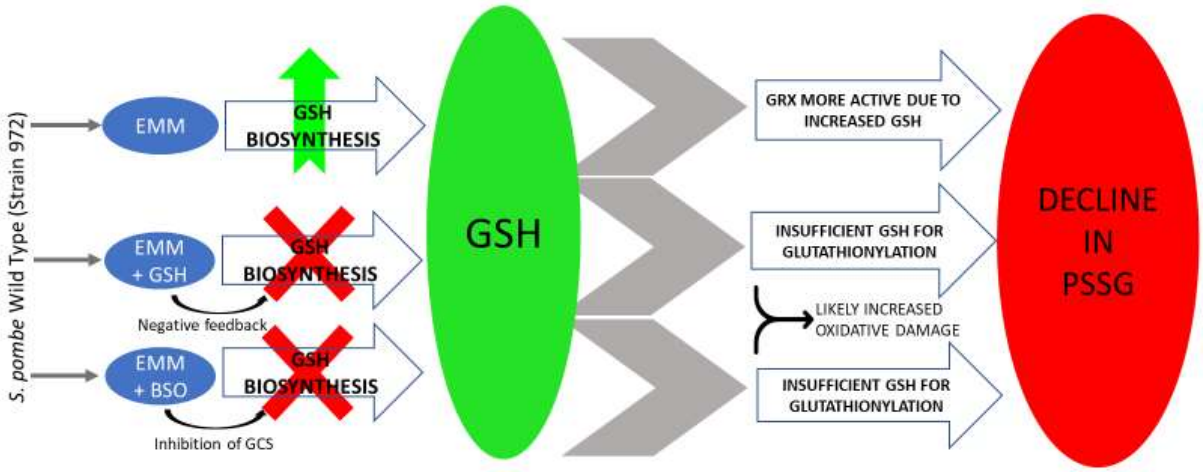

Figure 3.8 Summary of effects of aging under different growth conditions. *S. pombe was grown in minimal media (EMM) to prevent artefacts from complex media. In standard EMM, cells had a significant increase in intracellular GSH as they aged, which was possibly due to upregulation of GSH synthesis. With this increase in GSH, there was a decrease in glutathionylated protein (PSSG) as glutaredoxins were more active. In contrast, cells grown in EMM supplemented with GSH had a surprising decrease in GSH as the cells aged which is likely as a result of the synthesis of GSH being downregulated by negative feedback. Due to this lack of GSH in the system, there was a decline in PSSG. We suspect that there would be an associated increase in oxidative damage that should be measured in future studies. In cells grown in EMM with BSO, there is a drop in GSH which is expected because of BSO being a known inhibitor of GSH biosynthesis. However, PSSG levels remained the same.*

BSO treatment did decrease the free glutathione levels but there was no change in the protein glutathionylation levels. It is possible that the BSO was metabolized by the cells and therefore its effect was removed in these experiments. These confusing results could have another explanation. While it has generally been assumed that glutaredoxins act to deglutathionylate proteins, glutaredoxins could act to glutathionylate proteins (i.e.) they act as oxidases rather than just reductases (Ruoppolo et al., 1997; Lillig et al., 2008; Matsui et al., 2020). Thus, a loss of glutathione may prevent protein deglutathionylation.

These studies suggest that a more extensive set of assays should have been undertaken to characterize aging in *S. pombe*. It is possible that *S. pombe* strain 972 remains able to combat ROS antioxidant systems other than the glutaredoxin/glutathione system for longer periods of time. Therefore, the NADPH/NADP levels as well as protein oxidation and the glutaredoxin redox state should have been assessed which would yield a more comprehensive picture of the relationship between aging, glutathione levels the oxidation of glutaredoxins.

Chapter 4: General Discussion

Aging is a major risk factor for numerous diseases, including cancer, cardiovascular and neurodegenerative diseases and as global life expectancy increases, these age related diseases are becoming more prevalent (Niccoli and Partridge, 2012; Maluleke, 2018). Interestingly, these diseases have been linked to aging and three main pathways have been proposed, namely the nutrient sensing, mitochondrial dysfunction and DNA damage pathways (Niccoli and Partridge, 2012). ROS play a critical role in all three of these pathways which led to the hypothesis that exposure to ROS is increased or prolonged as cells age but this hypothesis has proved to be inconsistent and imprecise (Ristow, 2014).

We propose that there is a three-stage cellular response to ROS: exposure-detoxification, adaptation and post-stress recovery or repair (Section 1.4). Both the detoxification and adaptation stages have been well studied, but to date, post-stress recovery has been neglected. We hypothesized that failure of post-stress recovery, which occurs as the ROS levels begin to dissipate, is responsible for age-associated diseases. Testing this hypothesis required a mechanistic model and the glutaredoxin/glutathione system was a good candidate mechanism as GSH depletion, which is a key component of the adaptation stage, has been shown to be associated with neurodegenerative and cardiovascular diseases and with reduced autophagy which is associated with cancer (Guerrero-Gomez et al., 2019).

Computational modeling of the glutaredoxin/glutathione system was used as a first step to develop our understanding of the regulation of the system. Previously, our lab developed and validated a model of the dithiol mechanism of glutaredoxin activity (Pillay et al., 2009; Mashamaite et al., 2015a). However, other research groups have proposed the monothiol ping-pong model as the correct model of glutaredoxin activity (Begas et al., 2017; Deponte, 2017; Liedgens and Deponte, 2018). Here we show that the ping-pong model is inconsistent and is unable to predict independent glutaredoxin datasets. For this reason, we used the previously described dithiol model to test the glutaredoxin/glutathione system. Saturating the redox cycles of each reaction in the dithiol model confirmed that the system was dependent on the availability of GSH. This led to the hypothesis that the age-related decline in GSH may decrease in the activity of the glutaredoxin system and therefore

glutathionylated proteins would remain inactive which would contribute to the aging phenotype.

We first needed to show that there was indeed an age-associated increase in glutathionylation. *S. pombe* was a suitable model organism due to its simple redox networks and single dithiol glutaredoxin. Baseline free glutathione and glutathionylation levels in wild type (strain 972) *S. pombe* were determined after two days growth and compared with aged (5-day-old) cultures. Glutathione levels were tested using the well-established glutathione recycling assay (Baker et al., 1990) and glutathionylation levels were determined by cleaving glutathione from proteins using DTT and these glutathione concentrations were determined using the NDA assay (Menon and Board, 2013). Interestingly, the predicted age-related decline in free glutathione was not present and glutathionylation levels decreased with age which was in contrast to data obtained in fruit fly, rat and human cells (Sohal et al., 1990; Erden-İnal et al., 2002; Zhu et al., 2006; Ghezzi, 2013).

In future work, we propose raising glutaredoxin antibodies to track the performance of the glutaredoxin system and to determine the oxidized and reduced fractions of glutaredoxins. In addition, it would be beneficial to express all the components of the glutaredoxin/glutathione system to perform *in vitro* analysis of the effects of changes in glutathione concentration in a reconstituted system. Recently, it has been shown that the proposed role of ROS in aging and age-related disease may need to be modified. A study in mice has shown that thiol-based redox networks are remodeled differently in different tissues as cells age (Xiao et al., 2020). In light of this work, we believe that our hypothesis of aging in *S. pombe* will need to be modified to include network specific changes in addition to glutaredoxin and glutathione levels. Such analyses may be the key to delineating the role of post-stress recovery mechanisms to the antioxidant response and in disease.

References

Achilli, C., Ciana, A., and Minetti, G. (2015). The Discovery of Methionine Sulfoxide Reductase Enzymes: An Historical Account and Future Perspectives. Biofactors *41*, 135-152.

Adimora, N.J., Jones, D.P., and Kemp, M.L. (2010). A Model of Redox Kinetics Implicates the Thiol Proteome in Cellular Hydrogen Peroxide Responses. Antioxidants & redox signaling *13*, 731-743.

Aebi, H. (1984). [13] Catalase in Vitro. In Methods in Enzymology (Academic Press), pp. 121-126.

Arkun, Y., and Yasemi, M. (2018). Dynamics and Control of the Erk Signaling Pathway: Sensitivity, Bistability, and Oscillations. PloS one *13*, e0195513.

Åslund, F., Zheng, M., Beckwith, J., and Storz, G. (1999). Regulation of the Oxyr Transcription Factor by Hydrogen Peroxide and the Cellular Thiol—Disulfide Status. Proceedings of the National Academy of Sciences *96*, 6161-6165.

Atella, V., Piano Mortari, A., Kopinska, J., Belotti, F., Lapi, F., Cricelli, C., and Fontana, L. (2019). Trends in Age-Related Disease Burden and Healthcare Utilization. Aging Cell *18*, e12861.

Azadmanesh, J., and Borgstahl, G.E. (2018). A Review of the Catalytic Mechanism of Human Manganese Superoxide Dismutase. Antioxidants *7*, 25.

Baker, M.A., Cerniglia, G.J., and Zaman, A. (1990). Microtiter Plate Assay for the Measurement of Glutathione and Glutathione Disulfide in Large Numbers of Biological Samples. Analytical biochemistry *190*, 360-365.

Balazs, L., and Leon, M. (1994). Evidence of an Oxidative Challenge in the Alzheimer's Brain. Neurochemical research *19*, 1131-1137.

Ballatori, N., Krance, S.M., Notenboom, S., Shi, S., Tieu, K., and Hammond, C.L. (2009). Glutathione Dysregulation and the Etiology and Progression of Human Diseases. Biological chemistry *390*, 191-214.

Banerjee, R., Becker, D., Dickman, M., Gladyshev, V., and Ragsdale, S. (2008). Redox Biochemistry (Wiley Online Library).

Barnes, R.P., Fouquerel, E., and Opresko, P.L. (2019). The Impact of Oxidative DNA Damage and Stress on Telomere Homeostasis. Mechanisms of ageing and development *177*, 37-45.

Barrett, W.C., DeGnore, J.P., König, S., Fales, H.M., Keng, Y.-F., Zhang, Z.-Y., Yim, M.B., and Chock, P.B. (1999). Regulation of Ptp1b Via Glutathionylation of the Active Site Cysteine 215. Biochemistry *38*, 6699-6705.

Beckman, J.S., Estévez, A.G., Crow, J.P., and Barbeito, L. (2001). Superoxide Dismutase and the Death of Motoneurons in Als. Trends in neurosciences *24*, S15-S20.

Beckman, K.B., and Ames, B.N. (1998). The Free Radical Theory of Aging Matures. Physiological Reviews *78*, 547-581.

Begas, P., Liedgens, L., Moseler, A., Meyer, A.J., and Deponte, M. (2017). Glutaredoxin Catalysis Requires Two Distinct Glutathione Interaction Sites. Nature communications *8*, 1-13.

Begas, P., Staudacher, V., and Deponte, M. (2015). Systematic Re-Evaluation of the Bis (2-Hydroxyethyl) Disulfide (Heds) Assay Reveals an Alternative Mechanism and Activity of Glutaredoxins. Chemical science *6*, 3788-3796.

Benfeitas, R., Selvaggio, G., Antunes, F., Coelho, P.M., and Salvador, A. (2014). Hydrogen Peroxide Metabolism and Sensing in Human Erythrocytes: A Validated Kinetic Model and Reappraisal of the Role of Peroxiredoxin Ii. Free Radical Biology and Medicine *74*, 35-49.

Bennett, J.P. (2019). Medical Hypothesis: Neurodegenerative Diseases Arise from Oxidative Damage to Electron Tunneling Proteins in Mitochondria. Medical hypotheses *127*, 1-4.

Berlett, B.S., and Stadtman, E.R. (1997). Protein Oxidation in Aging, Disease, and Oxidative Stress. Journal of Biological Chemistry *272*, 20313-20316.

Berndt, C., Lillig, C.H., and Holmgren, A. (2008a). Thioredoxins and Glutaredoxins as Facilitators of Protein Folding. Biochimica et Biophysica Acta (BBA)-Molecular Cell Research *1783*, 641-650.

Berndt, C., Lillig, C.H., and Holmgren, A. (2008b). Thioredoxins and Glutaredoxins as Facilitators of Protein Folding. Biochimica et Biophysica Acta (BBA) - Molecular Cell Research *1783*, 641-650.

Bozonet, S.M., Findlay, V.J., Day, A.M., Cameron, J., Veal, E.A., and Morgan, B.A. (2005). Oxidation of a Eukaryotic 2-Cys Peroxiredoxin Is a Molecular Switch Controlling the Transcriptional Response to Increasing Levels of Hydrogen Peroxide. Journal of Biological Chemistry *280*, 23319-23327.

Bradley, M., Markesbery, W., and Lovell, M. (2010). Increased Levels of 4-Hydroxynonenal and Acrolein in the Brain in Preclinical Alzheimer Disease. Free Radical Biology and Medicine *48*, 1570-1576.

Brot, N., Fliss, H., Coleman, T., and Weissbach, H. (1984). Enzymatic Reduction of Methionine Sulfoxide Residues in Proteins and Peptides. In Methods in Enzymology (Academic Press), pp. 352-360.

Burton, G.J., and Jauniaux, E. (2011). Oxidative Stress. Best practice & research Clinical obstetrics & gynaecology *25*, 287-299.

Cattan, V., Mercier, N., Gardner, J.P., Regnault, V., Labat, C., Mäki-Jouppila, J., Nzietchueng, R., Benetos, A., Kimura, M., and Aviv, A. (2008). Chronic Oxidative Stress Induces a Tissue-Specific Reduction in Telomere Length in Cast/Ei Mice. Free Radical Biology and Medicine *44*, 1592-1598.

Cha, S.J., Kim, H., Choi, H.-J., Lee, S., and Kim, K. (2017). Protein Glutathionylation in the Pathogenesis of Neurodegenerative Diseases. Oxidative medicine and cellular longevity *2017*.

Chalissery, J., Jalal, D., Al-Natour, Z., and Hassan, A.H. (2017). Repair of Oxidative DNA Damage in Saccharomyces Cerevisiae. DNA repair *51*, 2-13.

Chen, B.-R., and Runge, K.W. (2009). A New Schizosaccharomyces Pombe Chronological Lifespan Assay Reveals That Caloric Restriction Promotes Efficient Cell Cycle Exit and Extends Longevity. Experimental gerontology *44*, 493-502.

Chen, G., Luo, Y., Warncke, K., Sun, Y., David, S.Y., Fu, H., Behera, M., Ramalingam, S.S., Doetsch, P.W., and Duong, D.M. (2019). Acetylation Regulates Ribonucleotide Reductase Activity and Cancer Cell Growth. Nature communications *10*, 1-16.

Chrestensen, C.A., Starke, D.W., and Mieyal, J.J. (2000). Acute Cadmium Exposure Inactivates Thioltransferase (Glutaredoxin), Inhibits Intracellular Reduction of Protein-Glutathionyl-Mixed Disulfides, and Initiates Apoptosis. Journal of Biological Chemistry *275*, 26556-26565.

Cleland, W. (1963). The Kinetics of Enzyme-Catalyzed Reactions with Two or More Substrates or Products: Ii. Inhibition: Nomenclature and Theory. Biochimica et Biophysica Acta (BBA)-Specialized Section on Enzymological Subjects *67*, 173-187.

Conway, D. (2019). Integrating in-Silico Models with in-Vitro Data to Generate Novel Insights into Biological Systems (Liverpool John Moores University).

Cotgreave, I.A., Gerdes, R., Schuppe-Koistinen, I., and Lind, C. (2002). [17] S-Glutathionylation of Glyceraldehyde-3-Phosphate Dehydrogenase: Role of Thiol Oxidation and Catalysis by Glutaredoxin. In Methods in Enzymology (Elsevier), pp. 175-182.

Das, A.B., Sadowska-Bartosz, I., Königstorfer, A., Kettle, A.J., and Winterbourn, C.C. (2018). Superoxide Dismutase Protects Ribonucleotide Reductase from Inactivation in Yeast. Free Radical Biology and Medicine *116*, 114-122.

Day, A.M., Brown, J.D., Taylor, S.R., Rand, J.D., Morgan, B.A., and Veal, E.A. (2012). Inactivation of a Peroxiredoxin by Hydrogen Peroxide Is Critical for Thioredoxin-Mediated Repair of Oxidized Proteins and Cell Survival. Molecular cell *45*, 398-408.

Dayer, R., Fischer, B.B., Eggen, R.I.L., and Lemaire, S.D. (2008). The Peroxiredoxin and Glutathione Peroxidase Families in ≪Em≫Chlamydomonas Reinhardtii≪/Em&Gt. Genetics *179*, 41.

De Belleroche, J., Orrell, R., and King, A. (1995). Familial Amyotrophic Lateral Sclerosis/Motor Neurone Disease (Fals): A Review of Current Developments. Journal of medical genetics *32*, 841.

Deepa, S.S., Van Remmen, H., Brooks, S.V., Faulkner, J.A., Larkin, L., McArdle, A., Jackson, M.J., Vasilaki, A., and Richardson, A. (2019). Accelerated Sarcopenia in Cu/Zn Superoxide Dismutase Knockout Mice. Free Radical Biology and Medicine *132*, 19-23.

Deponte, M. (2013). Glutathione Catalysis and the Reaction Mechanisms of Glutathione-Dependent Enzymes. Biochimica et Biophysica Acta (BBA)-General Subjects *1830*, 3217-3266.

Deponte, M. (2017). The Incomplete Glutathione Puzzle: Just Guessing at Numbers and Figures? Antioxidants & redox signaling *27*, 1130-1161.

Di Stefano, A., Frosali, S., Leonini, A., Ettorre, A., Priora, R., Di Simplicio, F.C., and Di Simplicio, P. (2006). Gsh Depletion, Protein S-Glutathionylation and Mitochondrial Transmembrane Potential Hyperpolarization Are Early Events in Initiation of Cell Death Induced by a Mixture of Isothiazolinones in Hl60 Cells. Biochimica et biophysica acta *1763*, 214-225.

Discola, K.F., de Oliveira, M.A., Cussiol, J.R.R., Monteiro, G., Bárcena, J.A., Porras, P., Padilla, C.A., Guimarães, B.G., and Netto, L.E.S. (2009). Structural Aspects of the Distinct Biochemical Properties of Glutaredoxin 1 and Glutaredoxin 2 from Saccharomyces Cerevisiae. Journal of molecular biology *385*, 889-901.

Djuika, C.F., Fiedler, S., Schnölzer, M., Sanchez, C., Lanzer, M., and Deponte, M. (2013). Plasmodium Falciparum Antioxidant Protein as a Model Enzyme for a Special Class of Glutaredoxin/Glutathione-Dependent Peroxiredoxins. Biochimica et Biophysica Acta (BBA)-General Subjects *1830*, 4073-4090.

Eckers, E., Bien, M., Stroobant, V., Herrmann, J.M., and Deponte, M. (2009). Biochemical Characterization of Dithiol Glutaredoxin 8 from Saccharomyces Cerevisiae: The Catalytic Redox Mechanism Redux. Biochemistry *48*, 1410-1423.

Erden-İnal, M., Sunal, E., and Kanbak, G. (2002). Age-Related Changes in the Glutathione Redox System. Cell biochemistry and function *20*, 61-66.

Fernandes, A.P., and Holmgren, A. (2004). Glutaredoxins: Glutathione-Dependent Redox Enzymes with Functions Far Beyond a Simple Thioredoxin Backup System. Antioxidants and Redox Signaling *6*, 63-74.

Flohe, L., Hecht, H., and Steinert, P. (1999). Glutathione and Trypanothione in Parasitic Hydroperoxide Metabolism. Free Radical Biology and Medicine *27*, 966-984.

Gallogly, M.M., Starke, D.W., Leonberg, A.K., Ospina, S.M.E., and Mieyal, J.J. (2008). Kinetic and Mechanistic Characterization and Versatile Catalytic Properties of Mammalian Glutaredoxin 2: Implications for Intracellular Roles. Biochemistry *47*, 11144-11157.

Gan, Z., Roerig, D.L., Clough, A.V., and Audi, S.H. (2011). Differential Responses of Targeted Lung Redox Enzymes to Rat Exposure to 60 or 85% Oxygen. Journal of Applied Physiology *111*, 95-107.

Ghezzi, P. (2013). Protein Glutathionylation in Health and Disease. Biochimica et Biophysica Acta (BBA)-General Subjects *1830*, 3165-3172.

Ghezzi, P., Jaquet, V., Marcucci, F., and Schmidt, H.H. (2017). The Oxidative Stress Theory of Disease: Levels of Evidence and Epistemological Aspects. British journal of pharmacology *174*, 1784-1796.

Gil, L., Siems, W., Mazurek, B., Gross, J., Schroeder, P., Voss, P., and Grune, T. (2006). Age-Associated Analysis of Oxidative Stress Parameters in Human Plasma and Erythrocytes. Free radical research *40*, 495-505.

Giustarini, D., Tsikas, D., Colombo, G., Milzani, A., Dalle-Donne, I., Fanti, P., and Rossi, R. (2016). Pitfalls in the Analysis of the Physiological Antioxidant Glutathione (Gsh) and Its Disulfide (Gssg) in Biological Samples: An Elephant in the Room. Journal of Chromatography B *1019*, 21-28.

Goth, L., and Eaton, J.W. (2000). Hereditary Catalase Deficiencies and Increased Risk of Diabetes. The Lancet *356*, 1820-1821.

Grant, C.M. (2001). Role of the Glutathione/Glutaredoxin and Thioredoxin Systems in Yeast Growth and Response to Stress Conditions. Molecular microbiology *39*, 533-541.

Guerrero-Gomez, D., Mora-Lorca, J.A., Saenz-Narciso, B., Naranjo-Galindo, F.J., Munoz-Lobato, F., Parrado-Fernandez, C., Goikolea, J., Cedazo-Minguez, Á., Link, C.D., and Neri, C.

(2019). Loss of Glutathione Redox Homeostasis Impairs Proteostasis by Inhibiting Autophagy-Dependent Protein Degradation. Cell Death & Differentiation *26*, 1545-1565.

Haeng-Im, J., Yuk-Young, L., Hye-Won, L., Ki-Sup, A., Eun-Hee, P., and Chang-Jin, L. (2002). Regulation of the Manganese-Containing Superoxide Dismutase Gene from Fission Yeast. Molecules & Cells (Springer Science & Business Media BV) *14*, 300.

Halliwell, B., and Gutteridge, J.M. (2015). Free Radicals in Biology and Medicine (Oxford University Press, USA).

Halliwell, B., and Whiteman, M. (2004). Measuring Rs and Oxidative Damage *in Vivo* and in Cell Culture: How Should You Do It and What Do the Results Mean? British Journal of Pharmacology *142*.

Harman, D. (1956). Aging: A Theory Based on Free Radical and Radiation Chemistry. Journal of Gerontology *11*, 298-300.

Hayles, J., and Nurse, P. (2018). Introduction to Fission Yeast as a Model System. Cold Spring Harbor Protocols *2018*, pdb. top079749.

Heit, C., Marshall, S., Singh, S., Yu, X., Charkoftaki, G., Zhao, H., Orlicky, D.J., Fritz, K.S., Thompson, D.C., and Vasiliou, V. (2017). Catalase Deletion Promotes Prediabetic Phenotype in Mice. Free Radical Biology and Medicine *103*, 48-56.

Holmgren, A. (1976). Hydrogen Donor System for Escherichia Coli Ribonucleoside-Diphosphate Reductase Dependent Upon Glutathione. Proceedings of the National Academy of Sciences *73*, 2275-2279.

Holmgren, A. (1989). Thioredoxin and Glutaredoxin Systems. Journal of Biological Chemistry *264*, 13963-13966.

Holmgren, A., Johansson, C., Berndt, C., Lönn, M., Hudemann, C., and Lillig, C. (2005). Thiol Redox Control Via Thioredoxin and Glutaredoxin Systems (Portland Press Limited).

Hugo, M., Trujillo, M., Piacenza, L., and Radi, R. (2018). Trypanothione Functions in Kinetoplastida. In Glutathione (CRC Press), pp. 307-314.

Humphries, K., Juliano, C., and Taylor, C. (2002). Regulation of Campdependent Protein Kinase Activity by Glutathionylation. Journal of Biological Chemistry *277*.

Huwaldt, J.A., and Steinhorst, S. (2013). Plot Digitizer. URL http://plotdigitizer sourceforge net.

Ighodaro, O., and Akinloye, O. (2018). First Line Defence Antioxidants-Superoxide Dismutase (Sod), Catalase (Cat) and Glutathione Peroxidase (Gpx): Their Fundamental Role in the Entire Antioxidant Defence Grid. Alexandria Journal of Medicine *54*, 287-293.

Indo, H.P., Yen, H.-C., Nakanishi, I., Matsumoto, K.-i., Tamura, M., Nagano, Y., Matsui, H., Gusev, O., Cornette, R., and Okuda, T. (2015). A Mitochondrial Superoxide Theory for Oxidative Stress Diseases and Aging. Journal of clinical biochemistry and nutrition *56*, 1-7.

Jain, K.K. (2017). Oxygen Toxicity. In Textbook of Hyperbaric Medicine (Springer), pp. 49-60.

Jeske, L., Placzek, S., Schomburg, I., Chang, A., and Schomburg, D. (2018). Brenda in 2019: A European Elixir Core Data Resource. Nucleic Acids Research *47*, D542-D549.

Kalinina, E., Chernov, N., and Saprin, A. (2008). Involvement of Thio-, Peroxi-, and Glutaredoxins in Cellular Redox-Dependent Processes. Biochemistry (Moscow) *73*, 1493-1510.

Kalyanaraman, B. (2013). Teaching the Basics of Redox Biology to Medical and Graduate Students: Oxidants, Antioxidants and Disease Mechanisms. Redox Biology *1*, 244-257.

Kamruzzaman, M., Choudhury, T.Z., Rahman, T., and Islam, L.N. (2019). A Cross-Sectional Study on Assessment of Oxidative Stress in Coronary Heart Disease Patients in Bangladesh. World Journal of Cardiovascular Diseases *9*, 331.

Kaya, A., Lobanov, A.V., Gerashchenko, M.V., Koren, A., Fomenko, D.E., Koc, A., and Gladyshev, V.N. (2014). Thiol Peroxidase Deficiency Leads to Increased Mutational Load and Decreased Fitness in Saccharomyces Cerevisiae. Genetics *198*, 905-917.

Kernodle, S.P., and Scandalios, J.G. (2001). Structural Organization, Regulation, and Expression of the Chloroplastic Superoxide Dismutase Sod1 Gene in Maize. Archives of Biochemistry and Biophysics *391*, 137-147.

Kim, S.O., Merchant, K., Nudelman, R., Beyer, W.F., Keng, T., DeAngelo, J., Hausladen, A., and Stamler, J.S. (2002). Oxyr: A Molecular Code for Redox-Related Signaling. Cell *109*, 383-396.

Klatt, P., Molina, E.P., and Lamas, S. (1999). Nitric Oxide Inhibits C-Jun DNA Binding by Specifically Targeteds-Glutathionylation. Journal of Biological Chemistry *274*, 15857-15864.

Kujoth, G.C., Hiona, A., Pugh, T.D., Someya, S., Panzer, K., Wohlgemuth, S.E., Hofer, T., Seo, A.Y., Sullivan, R., Jobling, W.A*., et al.* (2005). Mitochondrial DNA Mutations, Oxidative Stress, and Apoptosis in Mammalian Aging. Science *309*, 481.

Latimer, H.R., and Veal, E.A. (2016). Peroxiredoxins in Regulation of Mapk Signalling Pathways; Sensors and Barriers to Signal Transduction. Molecules and cells *39*, 40.

Le, D.T., Lee, B.C., Marino, S.M., Zhang, Y., Fomenko, D.E., Kaya, A., Hacioglu, E., Kwak, G.-H., Koc, A., and Kim, H.-Y. (2009). Functional Analysis of Free Methionine-R-

Sulfoxide Reductase from Saccharomyces Cerevisiae. Journal of Biological Chemistry *284*, 4354-4364.

Lee, J., Koo, N., and Min, D.B. (2004). Reactive Oxygen Species, Aging, and Antioxidative Nutraceuticals. Comprehensive Reviews in Food Science and Food Safety *3*, 21-33.

Li, W.-F., Yu, J., Ma, X.-X., Teng, Y.-B., Luo, M., Tang, Y.-J., and Zhou, C.-Z. (2010). Structural Basis for the Different Activities of Yeast Grx1 and Grx2. Biochimica et Biophysica Acta (BBA)-Proteins and Proteomics *1804*, 1542-1547.

Liao, B.-C., Hsieh, C.-W., Lin, Y.-C., and Wung, B.-S. (2010). The Glutaredoxin/Glutathione System Modulates Nf-Kb Activity by Glutathionylation of P65 in Cinnamaldehyde-Treated Endothelial Cells. Toxicological sciences *116*, 151-163.

Liedgens, L., and Deponte, M. (2018). The Catalytic Mechanism of Glutaredoxins. In Glutathione (CRC Press), pp. 251-261.

Liguori, I., Russo, G., Curcio, F., Bulli, G., Aran, L., Della-Morte, D., Gargiulo, G., Testa, G., Cacciatore, F., and Bonaduce, D. (2018). Oxidative Stress, Aging, and Diseases. Clinical interventions in aging *13*, 757.

Lillig, C.H., and Berndt, C. (2013). Glutaredoxins in Thiol/Disulfide Exchange. Antioxidants & redox signaling *18*, 1654-1665.

Lillig, C.H., Berndt, C., and Holmgren, A. (2008). Glutaredoxin Systems. Biochimica et Biophysica Acta (BBA)-General Subjects *1780*, 1304-1317.

Lind, C., Gerdes, R., Schuppe-Koistinen, I., and Cotgreave, I.A. (1998). Studies on the Mechanism of Oxidative Modification of Human Glyceraldehyde-3-Phosphate Dehydrogenase by Glutathione: Catalysis by Glutaredoxin. Biochemical and Biophysical Research Communications *247*, 481-486.

Longo, V.D., Liou, L.-L., Valentine, J.S., and Gralla, E.B. (1999). Mitochondrial Superoxide Decreases Yeast Survival in Stationary Phase. Archives of Biochemistry and Biophysics *365*, 131-142.

Mailloux, R.J., Gill, R., and Young, A. (2020). Protein S-Glutathionylation and the Regulation of Cellular Functions. In Oxidative Stress (Elsevier), pp. 217-247.

Maluleke, R. (2018). Mortality and Causes of Death in South Africa, 2016: Findings from Death Notification, S.S. Africa, ed. (Pretoria: Government of the Republic of South Africa), pp. 20-36.

Marguerat, S., Schmidt, A., Codlin, S., Chen, W., Aebersold, R., and Bähler, J. (2012). Quantitative Analysis of Fission Yeast Transcriptomes and Proteomes in Proliferating and Quiescent Cells. Cell *151*, 671-683.

Mashamaite, Lefentse N., Rohwer, Johann M., and Pillay, Ché S. (2015a). The Glutaredoxin Mono- and Di-Thiol Mechanisms for Deglutathionylation Are Functionally Equivalent: Implications for Redox Systems Biology. Bioscience Reports *35*, e00173.

Mashamaite, L.N., Rohwer, J.M., and Pillay, C.S. (2015b). The Glutaredoxin Mono-and Di-Thiol Mechanisms for Deglutathionylation Are Functionally Equivalent: Implications for Redox Systems Biology. Bioscience reports *35*, e00173.

Matsui, R., Ferran, B., Oh, A., Croteau, D., Shao, D., Han, J., Pimentel, D.R., and Bachschmid, M.M. (2020). Redox Regulation Via Glutaredoxin-1 and Protein S-Glutathionylation. Antioxidants & Redox Signaling *32*, 677-700.

Matsuyama, A., Arai, R., Yashiroda, Y., Shirai, A., Kamata, A., Sekido, S., Kobayashi, Y., Hashimoto, A., Hamamoto, M., and Hiraoka, Y. (2006). Orfeome Cloning and Global Analysis of Protein Localization in the Fission Yeast Schizosaccharomyces Pombe. Nature biotechnology *24*, 841-847.

McCance, D.R., Holmes, V.A., Maresh, M.J.A., Patterson, C.C., Walker, J.D., Pearson, D.W.M., and Young, I.S. (2010). Vitamins C and E for Prevention of Pre-Eclampsia in Women with Type 1 Diabetes (Dapit): A Randomised Placebo-Controlled Trial. The Lancet *376*, 259-266.

Medley, J.K. (2019). Towards a Scalable, Future-Proof Platform for Dynamical Modeling in Biology.

Menon, D., and Board, P.G. (2013). A Fluorometric Method to Quantify Protein Glutathionylation Using Glutathione Derivatization with 2, 3-Naphthalenedicarboxaldehyde. Analytical biochemistry *433*, 132-136.

Mieyal, J.J., Gallogly, M.M., Qanungo, S., Sabens, E.A., and Shelton, M.D. (2008). Molecular Mechanisms and Clinical Implications of Reversible Protein S-Glutathionylation. Antioxidants & redox signaling *10*, 1941-1988.

Mills, G.C. (1957). Hemoglobin Catabolism I. Glutathione Peroxidase, an Erythrocyte Enzyme Which Protects Hemoglobin from Oxidative Breakdown. Journal of Biological Chemistry *229*, 189-197.

Molina, M.M., Bellí, G., de la Torre, M.A., Rodríguez-Manzaneque, M.T., and Herrero, E. (2004). Nuclear Monothiol Glutaredoxins of Saccharomyces Cerevisiae Can Function as Mitochondrial Glutaredoxins. Journal of Biological Chemistry *279*, 51923-51930.

Möller, M.N., Cuevasanta, E., Orrico, F., Lopez, A.C., Thomson, L., and Denicola, A. (2019). Diffusion and Transport of Reactive Species across Cell Membranes. In Bioactive Lipids in Health and Disease (Springer), pp. 3-19.

Morabito, R., Remigante, A., and Marino, A. (2019). Melatonin Protects Band 3 Protein in Human Erythrocytes against H2o2-Induced Oxidative Stress. Molecules *24*, 2741.

Morris, G., Anderson, G., Dean, O., Berk, M., Galecki, P., Martin-Subero, M., and Maes, M. (2014a). The Glutathione System: A New Drug Target in Neuroimmune Disorders. Mol Neurobiol Molecular Neurobiology *50*, 1059-1084.

Morris, G., Anderson, G., Dean, O., Berk, M., Galecki, P., Martin-Subero, M., and Maes, M. (2014b). The Glutathione System: A New Drug Target in Neuroimmune Disorders. Molecular Neurobiology *50*, 1059-1084.

Moskovitz, J., Bar-Noy, S., Williams, W.M., Requena, J., Berlett, B.S., and Stadtman, E.R. (2001). Methionine Sulfoxide Reductase (Msra) Is a Regulator of Antioxidant Defense and Lifespan in Mammals. Proceedings of the National Academy of Sciences *98*, 12920.

Moskovitz, J., Berlett, B.S., Poston, J.M., and Stadtman, E.R. (1997). The Yeast Peptide-Methionine Sulfoxide Reductase Functions as an Antioxidant in Vivo. Proceedings of the National Academy of Sciences *94*, 9585-9589.

Moskovitz, J., Poston, J.M., Berlett, B.S., Nosworthy, N.J., Szczepanowski, R., and Stadtman, E.R. (2000). Identification and Characterization of a Putative Active Site for Peptide Methionine Sulfoxide Reductase (Msra) and Its Substrate Stereospecificity. Journal of Biological Chemistry *275*, 14167-14172.

Muller, F.L., Song, W., Liu, Y., Chaudhuri, A., Pieke-Dahl, S., Strong, R., Huang, T.-T., Epstein, C.J., Roberts II, L.J., and Csete, M. (2006). Absence of Cuzn Superoxide Dismutase Leads to Elevated Oxidative Stress and Acceleration of Age-Dependent Skeletal Muscle Atrophy. Free Radical Biology and Medicine *40*, 1993-2004.

Netto, L.E., and Antunes, F. (2016). The Roles of Peroxiredoxin and Thioredoxin in Hydrogen Peroxide Sensing and in Signal Transduction. Molecules and cells *39*, 65.

Newman, S.F., Sultana, R., Perluigi, M., Coccia, R., Cai, J., Pierce, W.M., Klein, J.B., Turner, D.M., and Butterfield, D.A. (2007). An Increase in S-Glutathionylated Proteins in the Alzheimer's Disease Inferior Parietal Lobule, a Proteomics Approach. Journal of neuroscience research *85*, 1506-1514.

Niccoli, T., and Partridge, L. (2012). Ageing as a Risk Factor for Disease. Current biology *22*, R741-R752.

Nonaka, K., Kume, N., Urata, Y., Seto, S., Kohno, T., Honda, S., Ikeda, S., Muroya, T., Ikeda, Y., and Ihara, Y. (2007). Serum Levels of S-Glutathionylated Proteins as a Risk-Marker for Arteriosclerosis Obliterans. Circulation Journal *71*, 100-105.

Olivier, B.G., Rohwer, J.M., and Hofmeyr, J.-H.S. (2005). Modelling Cellular Systems with Pysces. Bioinformatics *21*, 560-561.

Orwar, O., Fishman, H.A., Ziv, N.E., Scheller, R.H., and Zare, R.N. (1995). Use of 2, 3-Naphthalenedicarboxaldehyde Derivatization for Single-Cell Analysis of Glutathione by Capillary Electrophoresis and Histochemical Localization by Fluorescence Microscopy. Analytical chemistry *67*, 4261-4268.

Paulo, E., García-Santamarina, S., Calvo, I.A., Carmona, M., Boronat, S., Domènech, A., Ayté, J., and Hidalgo, E. (2014). A Genetic Approach to Study H 2 O 2 Scavenging in Fission Yeast–Distinct Roles of Peroxiredoxin and Catalase. Molecular microbiology *92*, 246-257.

Peltoniemi, M.J., Karala, A.-R., Jurvansuu, J.K., Kinnula, V.L., and Ruddock, L.W. (2006). Insights into Deglutathionylation Reactions: Different Intermediates in the Glutaredoxin and Protein Disulfide Isomerase Catalyzed Reactions Are Defined by the Γ-Linkage Present in Glutathione. Journal of Biological Chemistry *281*, 33107-33114.

Perkins, A., Nelson, K.J., Parsonage, D., Poole, L.B., and Karplus, P.A. (2015). Peroxiredoxins: Guardians against Oxidative Stress and Modulators of Peroxide Signaling. Trends in Biochemical Sciences *40*, 435-445.

Peskin, A.V., Dickerhof, N., Poynton, R.A., Paton, L.N., Pace, P.E., Hampton, M.B., and Winterbourn, C.C. (2013a). Hyperoxidation of Peroxiredoxins 2 and 3 Rate Constants for the Reactions of the Sulfenic Acid of the Peroxidatic Cysteine. Journal of Biological Chemistry *288*, 14170-14177.

Peskin, A.V., Dickerhof, N., Poynton, R.A., Paton, L.N., Pace, P.E., Hampton, M.B., and Winterbourn, C.C. (2013b). Hyperoxidation of Peroxiredoxins 2 and 3: Rate Constants for the Reactions of the Sulfenic Acid of the Peroxidatic Cysteine. Journal of Biological Chemistry *288*, 14170-14177.

Peskin, A.V., Low, F.M., Paton, L.N., Maghzal, G.J., Hampton, M.B., and Winterbourn, C.C. (2007). The High Reactivity of Peroxiredoxin 2 with H2o2 Is Not Reflected in Its Reaction with Other Oxidants and Thiol Reagents. Journal of Biological Chemistry *282*, 11885-11892.

Peskin, A.V., Pace, P.E., Behring, J.B., Paton, L.N., Soethoudt, M., Bachschmid, M.M., and Winterbourn, C.C. (2016). Glutathionylation of the Active Site Cysteines of Peroxiredoxin 2 and Recycling by Glutaredoxin. Journal of Biological Chemistry *291*, 3053-3062.

Pillay, C.S., Eagling, B.D., Driscoll, S.R., and Rohwer, J.M. (2016). Quantitative Measures for Redox Signaling. Free Radical Biology and Medicine *96*, 290-303.

Pillay, C.S., Hofmeyr, J.-H., Mashamaite, L.N., and Rohwer, J.M. (2013). From Top-Down to Bottom-Up: Computational Modeling Approaches for Cellular Redoxin Networks. Antioxidants & Redox Signaling *18*, 2075-2086.

Pillay, C.S., Hofmeyr, J.-H.S., Olivier, B.G., Snoep, J.L., and Rohwer, J.M. (2009). Enzymes or Redox Couples? The Kinetics of Thioredoxin and Glutaredoxin Reactions in a Systems Biology Context. Biochemical Journal *417*, 269-277.

Pinto, M., Neves, J., Palha, M., and Bicho, M. (2002). Oxidative Stress in Portuguese Children with Down Syndrome. Down Syndrome Research and Practice *8*, 79-82.

Porqué, P.G., Baldesten, A., and Reichard, P. (1970). The Involvement of the Thioredoxin System in the Reduction of Methionine Sulfoxide and Sulfate. Journal of Biological Chemistry *245*, 2371-2374.

Radyuk, S.N., and Orr, W.C. (2018). The Multifaceted Impact of Peroxiredoxins on Aging and Disease. Antioxidants & redox signaling *29*, 1293-1311.

Rahman, I., and MacNee, W. (2000). Oxidative Stress and Regulation of Glutathione in Lung Inflammation. European Respiratory Journal *16*, 534-554.

Ravichandran, V., Seres, T., Moriguchi, T., Thomas, J.A., and Johnston, R. (1994). S-Thiolation of Glyceraldehyde-3-Phosphate Dehydrogenase Induced by the Phagocytosis-Associated Respiratory Burst in Blood Monocytes. Journal of Biological Chemistry *269*, 25010-25015.

Reyes, A.M., Pedre, B., De Armas, M.I., Tossounian, M.-A., Radi, R., Messens, J., and Trujillo, M. (2018). Chemistry and Redox Biology of Mycothiol. Antioxidants & redox signaling *28*, 487-504.

Rhee, S.G. (2016). Overview on Peroxiredoxin. Molecules and cells *39*, 1-5.

Rhee, S.G., Yang, K.-S., Kang, S.W., Woo, H.A., and Chang, T.-S. (2005). Controlled Elimination of Intracellular H2o2: Regulation of Peroxiredoxin, Catalase, and Glutathione Peroxidase Via Post-Translational Modification. Antioxidants & redox signaling *7*, 619-626.

Ristow, M. (2014). Unraveling the Truth About Antioxidants: Mitohormesis Explains Ros-Induced Health Benefits. Nature medicine *20*, 709-711.

Ruoppolo, M., Lundström-Ljung, J., Talamo, F., Pucci, P., and Marino, G. (1997). Effect of Glutaredoxin and Protein Disulfide Isomerase on the Glutathione-Dependent Folding of Ribonuclease A. Biochemistry *36*, 12259-12267.

Schafer, F.Q., and Buettner, G.R. (2001). Redox Environment of the Cell as Viewed through the Redox State of the Glutathione Disulfide/Glutathione Couple. Free radical biology and medicine *30*, 1191-1212.

Shi, J., Vlamis-Gardikas, A., Aslund, F., Holmgren, A., and Rosen, B.P. (1999). Reactivity of Glutaredoxins 1, 2, and 3 from Escherichia Coli Shows That Glutaredoxin 2 Is the Primary Hydrogen Donor to Arsc-Catalyzed Arsenate Reduction. The Journal of biological chemistry *274*, 36039-36042.

Sies, H. (2018). On the History of Oxidative Stress: Concept and Some Aspects of Current Development. Current Opinion in Toxicology *7*, 122-126.

Sies, H., Berndt, C., and Jones, D.P. (2017). Oxidative Stress. Annual review of biochemistry *86*, 715-748.

Sirover, M.A. (2017). Gapdh: A Multifunctional Moonlighting Protein in Eukaryotes and Prokaryotes. Moonlighting Proteins: Novel Virulence Factors in Bacterial Infections, 147-167.

Sohal, R., Arnold, L., and Orr, W.C. (1990). Effect of Age on Superoxide Dismutase, Catalase, Glutathione Reductase, Inorganic Peroxides, Tba-Reactive Material, Gsh/Gssg, Nadph/Nadp+ and Nadh/Nad+ in Drosophila Melanogaster. Mechanisms of ageing and development *56*, 223-235.

Srinivasan, U., Mieyal, P.A., and Mieyal, J.J. (1997). Ph Profiles Indicative of Rate-Limiting Nucleophilic Displacement in Thioltransferase Catalysis. Biochemistry *36*, 3199-3206.

Srour, M., Bilto, Y., Juma, M., and Irhimeh, M. (2000). Exposure of Human Erythrocytes to Oxygen Radicals Causes Loss of Deformability, Increased Osmotic Fragility, Lipid Peroxidation and Protein Degradation. Clinical hemorheology and microcirculation *23*, 13-21.

Stöcker, S., Van Laer, K., Mijuskovic, A., and Dick, T.P. (2018). The Conundrum of Hydrogen Peroxide Signaling and the Emerging Role of Peroxiredoxins as Redox Relay Hubs. Antioxidants & redox signaling *28*, 558-573.

Tanaka, T., Izawa, S., and Inoue, Y. (2005). Gpx2, Encoding a Phospholipid Hydroperoxide Glutathione Peroxidase Homologue, Codes for an Atypical 2-Cys Peroxiredoxin in Saccharomyces Cerevisiae. Journal of Biological Chemistry *280*, 42078-42087.

Tarrago, L., and Gladyshev, V. (2012). Recharging Oxidative Protein Repair: Catalysis by Methionine Sulfoxide Reductases Towards Their Amino Acid, Protein, and Model Substrates. Biochemistry (Moscow) *77*, 1097-1107.

Tietze, F. (1969). Enzymic Method for Quantitative Determination of Nanogram Amounts of Total and Oxidized Glutathione: Applications to Mammalian Blood and Other Tissues. Analytical biochemistry *27*, 502-522.

Toledano, M.B., and Huang, M.-E. (2017). The Unfinished Puzzle of Glutathione Physiological Functions, an Old Molecule That Still Retains Many Enigmas (Mary Ann Liebert, Inc. 140 Huguenot Street, 3rd Floor New Rochelle, NY 10801 USA).

Toledano, M.B., Kumar, C., Le Moan, M., Spector, D., and Tacnet, F. (2007). The System Biology of Thiol Redox System in Escherichia Coli and Yeast: Differential Functions in Oxidative Stress, Iron Metabolism and DNA Sythesis. FEBS Letters *581*, 3598-3607.

Tomalin, L.E., Day, A.M., Underwood, Z.E., Smith, G.R., Dalle Pezze, P., Rallis, C., Patel, W., Dickinson, B.C., Bähler, J., and Brewer, T.F. (2016). Increasing Extracellular H2o2 Produces a Bi-Phasic Response in Intracellular H2o2, with Peroxiredoxin Hyperoxidation Only Triggered Once the Cellular H2o2-Buffering Capacity Is Overwhelmed. Free Radical Biology and Medicine *95*, 333-348.

Traber, M.G., and Stevens, J.F. (2011). Vitamins C and E: Beneficial Effects from a Mechanistic Perspective. Free Radical Biology and Medicine *51*, 1000-1013.

Trujillo, M., Clippe, A., Manta, B., Ferrer-Sueta, G., Smeets, A., Declercq, J.-P., Knoops, B., and Radi, R. (2007). Pre-Steady State Kinetic Characterization of Human Peroxiredoxin 5: Taking Advantage of Trp84 Fluorescence Increase Upon Oxidation. Archives of Biochemistry and Biophysics *467*, 95-106.

Tsopanakis, A.D., and Herries, D.G. (1975). Kinetic Discrimination between Two Types of Enzyme Mechanism: Application to Lactose Synthetase. European Journal of Biochemistry *53*, 193-196.

Tubbs, A., and Nussenzweig, A. (2017). Endogenous DNA Damage as a Source of Genomic Instability in Cancer. Cell *168*, 644-656.

Venkateshappa, C., Harish, G., Mahadevan, A., Bharath, M.S., and Shankar, S. (2012). Elevated Oxidative Stress and Decreased Antioxidant Function in the Human Hippocampus and Frontal Cortex with Increasing Age: Implications for Neurodegeneration in Alzheimer's Disease. Neurochemical research *37*, 1601-1614.

Vivancos, A.P., Castillo, E.A., Biteau, B., Nicot, C., Ayté, J., Toledano, M.B., and Hidalgo, E. (2005). A Cysteine-Sulfinic Acid in Peroxiredoxin Regulates H2o2-Sensing by the Antioxidant Pap1 Pathway. Proceedings of the National Academy of Sciences *102*, 8875-8880.

Wang, J., Boja, E.S., Tan, W., Tekle, E., Fales, H.M., English, S., Mieyal, J.J., and Chock, P.B. (2001). Reversible Glutathionylation Regulates Actin Polymerization in A431 Cells. Journal of Biological Chemistry *276*, 47763-47766.

Wentzel, P., Ejdesjö, A., and Eriksson, U.J. (2003). Maternal Diabetes in Vivo and High Glucose in Vitro Diminish Gapdh Activity in Rat Embryos. Diabetes *52*, 1222-1228.

Wilcox, K.C., Zhou, L., Jordon, J.K., Huang, Y., Yu, Y., Redler, R.L., Chen, X., Caplow, M., and Dokholyan, N.V. (2009). Modifications of Superoxide Dismutase (Sod1) in Human

Erythrocytes a Possible Role in Amyotrophic Lateral Sclerosis. Journal of Biological Chemistry *284*, 13940-13947.

Winterbourn, C.C. (2008). Reconciling the Chemistry and Biology of Reactive Oxygen Species. Nature chemical biology *4*, 278.

Winterbourn, C.C. (2019). Regulation of Intracellular Glutathione. Redox biology *22*.

Winterbourn, C.C., and Metodiewa, D. (1999). Reactivity of Biologically Important Thiol Compounds with Superoxide and Hydrogen Peroxide. Free Radical Biology and Medicine *27*, 322-328.

Wong, C.-M., Siu, K.-L., and Jin, D.-Y. (2004). Peroxiredoxin-Null Yeast Cells Are Hypersensitive to Oxidative Stress and Are Genomically Unstable. Journal of Biological Chemistry *279*, 23207-23213.

Xiao, H., Jedrychowski, M.P., Schweppe, D.K., Huttlin, E.L., Yu, Q., Heppner, D.E., Li, J., Long, J., Mills, E.L., and Szpyt, J. (2020). A Quantitative Tissue-Specific Landscape of Protein Redox Regulation During Aging. Cell.

Xie, Y., Kole, S., Precht, P., Pazin, M.J., and Bernier, M. (2008). S-Glutathionylation Impairs Signal Transducer and Activator of Transcription 3 Activation and Signaling. Endocrinology *150*, 1122-1131.

Yamakura, F., and Kawasaki, H. (2010). Post-Translational Modifications of Superoxide Dismutase. Biochimica et Biophysica Acta (BBA)-Proteins and Proteomics *1804*, 318-325.

Zabel, M., Nackenoff, A., Kirsch, W.M., Harrison, F.E., Perry, G., and Schrag, M. (2018). Markers of Oxidative Damage to Lipids, Nucleic Acids and Proteins and Antioxidant Enzymes Activities in Alzheimer's Disease Brain: A Meta-Analysis in Human Pathological Specimens. Free Radical Biology and Medicine *115*, 351-360.

Zhao, R.Z., Jiang, S., Zhang, L., and Yu, Z.B. (2019). Mitochondrial Electron Transport Chain, Ros Generation and Uncoupling. International journal of molecular medicine *44*, 3-15.

Zhu, Y., Carvey, P.M., and Ling, Z. (2006). Age-Related Changes in Glutathione and Glutathione-Related Enzymes in Rat Brain. Brain research *1090*, 35-44.

Zuin, A., Carmona, M., Morales-Ivorra, I., Gabrielli, N., Vivancos, A.P., Ayté, J., and Hidalgo, E. (2010). Lifespan Extension by Calorie Restriction Relies on the Sty1 Map Kinase Stress Pathway. The EMBO Journal *29*, 981-991.

Appendices

Appendix A

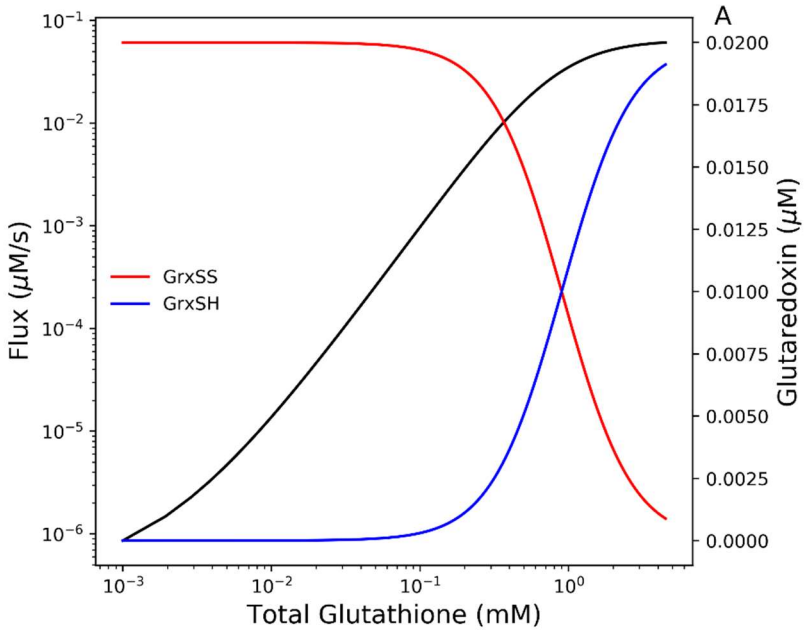

Figure S2.1: Saturating the redox cycles in the reduction of GrxSS by glutathione. *Increasing the total glutathione (B) both resulted in increased active GrxSH. Reaction conditions: PSSG (5μM), GR (20nM) and NADPH (50μM). Glutathione and flux plotted in logscale.*

Appendix B

PySCeS Models

```
#Model units: uM, s

FIX: PSSG PSH NADPH NADP GSHp

R1: GSSG + NADPH = 2 GSH + NADP

    kcat1*GR*GSSG*NADPH/(Kgssg*Knadph)/((1+GSSG/Kgssg)
*(1+NADPH/Knadph))

    #kcat1*GR*GSSG*NADPH/(Kgssg*Knadph)/((1+GSSG/Kgssg)
*(1+NADPH/Knadph+NADP/Knadp))


R2: GrxSS + 2 GSH = GrxSH + GSSG

   k2*GrxSS*(GSH**2) *(1-((GSSG*GrxSH)/(GrxSS*GSH*GSH))/Keq2)


#k2*(GrxSS*(GSH**2) - (GrxSH*GSSG)/Keq2)


R3: GrxSH + PSSG = GrxSS + PSH + GSHp

   k3*GrxSH*PSSG

#Rate parameters

kcat1=500

GR    = 0.02   # 20 nM GR

Kgssg = 55

Knadph = 3.8

GSHp   = 1

Knadp = 55
```

k2 = 4.77673309454e-006

Keq2 = 1.3656e-6 # NB. Units: per micromolar (uM)^-1

k3 = 0.640964271921

#Metabolites (uM)

#fixed

NADPH = 50

NADP = 1

PSSG = 5

PSH = 1

#variable

GrxSS = 0.01

GrxSH = 0.01

GSH = 998 # total GSH monomer = 1 mM

GSSG = 1

Appendix C

In Vivo Data

Table S3.1 Optical density at 600 nm of S. Pombe cells grown in different media

Growth Conditions	EMM		EMM + 1 mM GSH		EMM + 1 mM BSO	
	2 DAY	5 DAY	2 DAY	5 DAY	2 DAY	5 DAY
Average OD_{600}	2.09	2.488	1.56	2.16	1.45	2.16
Standard Deviation	0.027	0.296	0.767	0.011	0.621	0.034
Standard Error	0.016	0.171	0.443	0.007	0.358	0.020

Table S3.2 Average A_{405nm} of known glutathione concentrations

GSH Concentration (µM)	Average $A_{405\ nm}$	Standard Deviation	Standard Error
0	0.05337	0.0006	0.0003
10.2	0.0665	0.0071	0.0041
20.3	0.0700	0.0026	0.0015
40.6	0.0865	0.0049	0.0028
81.3	0.1168	0.0013	0.0008
162.5	0.1929	0.0103	0.0060
325.0	0.2942	0.0114	0.0066

Table S3.3: Glutathione concentrations of *S. pombe* under different growth conditions

Growth conditions	EMM		EMM + 1 mM GSH		EMM + 1 mM BSO	
	2 DAY	5 DAY	2 DAY	5 DAY	2 DAY	5 DAY
Corrected Glutathione Concentration (µM/20µL)	36.62	43.09	55.67	34.55	44.34	32.86
Standard Deviation	8.76	22.14	18.83	6.25	12.15	8.76
Standard Error	3.58	9.04	7.69	2.55	4.96	3.58

Table S3.5: Protein concentrations of *S. pombe* grown in different conditions

Growth conditions	EMM		EMM + 1 mM GSH		EMM + 1 mM BSO	
	2 DAY	5 DAY	2 DAY	5 DAY	2 DAY	5 DAY
Protein Concentration (mg/mL)	0,27	0,377	0,188	0,439	0,196	0,335
Standard Deviation	0,459	0,41	0,21	0,511	0,155	0,405
Standard Error	0,153	0,137	0,07	0,17	0,052	0,135

Table S3.6: NDA assay of known glutathione concentrations

GSH Concentration (µg/mL)	Average Fluorescence (AU)	Standard Deviation	Standard Error
0.16	0,67	1,16	0,67
0.33	1	1	0,58
0.65	1	0	0
1.30	1,33	0,58	0,33

Table S3.5 Concentration of Cleaved Glutathione per mg/mL Protein from S. pombe cultures grown in different media

Growth Conditions	EMM		EMM + 1 mM GSH		EMM + 1 mM BSO	
	2 DAY	5 DAY	2 DAY	5 DAY	2 DAY	5 DAY
Glutathione Concentration (µM)	3348,814	1620,155	7086,507	2193,577	6005,678	3126,731
Standard Deviation	734,931	833,333	833,333	833,333	555,555	878,410
Standard Error	244,977	277,778	277,778	277,778	185,185	292,803